Baseline Inflammatory Profiles in Moderate-to-Severe Depression and Differential Response to Intermittent Theta-Burst Stimulation

Bruno Pedraz-Petrozzi[1,2,3,4,*], Jonas Wilkening[5], Nicole Ziegler[6], Martijn Arns[7,8], Alexander Sartorius[1,2,4], Roberto Goya-Maldonado[5]

[1]Department of Psychiatry and Psychotherapy, Central Institute of Mental Health, Medical Faculty Mannheim, University of Heidelberg, Mannheim, Germany.
[2]German Center for Mental Health (DZPG), partner site Mannheim, Germany.
[3]Research Group of Stress-related Disorders, Department of Psychiatry and Psychotherapy, Central Institute of Mental Health, Clinical Faculty Mannheim, University of Heidelberg, Mannheim, Germany
[4]Research Group Brain Stimulation, Department of Psychiatry and Psychotherapy, Central Institute of Mental Health, Clinical Faculty Mannheim, University of Heidelberg, Mannheim, Germany
[5]Laboratory of Systems Neuroscience and Imaging in Psychiatry (SNIP-Lab), Department of Psychiatry and Psychotherapy, University Medical Center Göttingen, Göttingen, Germany
[6]Fraunhofer Institute for Translational Medicine and Pharmacology ITMP, Frankfurt am Main, Germany
[7]Brainclinics Foundation, Nijmegen, The Netherlands
[8]Stanford Brain Stimulation Lab, Stanford University, Palo Alto, United States of America.

***Corresponding author:**

Dr. Bruno Pedraz-Petrozzi, Ph.D.
Central Institute of Mental Health (CIMH)
Department of Psychiatry and Psychotherapy
J5
D-68159 Mannheim
Germany
Phone: +49 621 1703 4363
Email: bruno.pedraz@zi-mannheim.de
ORCID: 0000-0002-4119-971X

Authors' ORCID
Jonas Wilkening, ORCID: 0009-0000-3539-1900
Nicole Ziegler, ORCID: 0009-0002-4626-8793
Martjin Arns, ORCID: 0000-0002-0610-7613
Alexander Sartorius, ORCID: 0000-0002-1243-3693
Roberto Goya-Maldonado, ORCID: 0000-0002-7368-1332

Abstract Word Count: 238 words; **Total Word Count**: 4942 words

Keywords (MeSH terms): Major Depressive Disorder; Inflammation; rTMS; iTBS; Cytokines; Biomarkers; Treatment Response; Clustering Analysis; Immune Dysregulation.

ABSTRACT

Major depressive disorder (MDD) is a biologically heterogeneous condition, with a subset of patients exhibiting elevated inflammatory markers associated with greater symptom burden and lower responsiveness to antidepressants. Treatment outcomes with repetitive transcranial magnetic stimulation (rTMS) are also highly variable, and inflammation may impair neuroplasticity, thereby modulating treatment efficacy. This exploratory study investigated whether baseline inflammatory protein signatures could influence the response to intermittent theta burst stimulation (iTBS). Using the Olink® Target 96 Inflammation panel, baseline inflammatory protein levels were analyzed in 54 patients with moderate-to-severe depression (baseline MADRS ≥20) undergoing iTBS treatment. K-means clustering identified two subgroups: Cluster 1 (n = 28) and Cluster 2 (n = 26). Cluster 2 showed the highest proportion of responders, whereas Cluster 1 showed the lowest. The clusters did not differ significantly in age, sex, medication status, randomization arm, or body mass index. Differential protein expression was assessed using volcano plots with false discovery rate (FDR) correction. Pathway enrichment analyses using Kyoto Encyclopedia of Genes and Genomes (KEGG) and Reactome databases identified biological processes associated with the clustering solution. Volcano analysis identified 10 differentially expressed proteins between clusters (FDR < 0.05 and |ΔNPX| ≥ 1). Enrichment analyses implicated cytokine–cytokine receptor interaction, chemokine signaling, and interleukin signaling pathways as characteristic of the lower-response subgroup. These findings indicate that baseline inflammatory signatures may help differentiate responsiveness to iTBS in moderate-to-severe depression, supporting future pathway investigations as a potential strategy for personalized psychiatry.

Keywords (MeSH terms): Major Depressive Disorder; Inflammation; rTMS; iTBS; Cytokines; Biomarkers; Treatment Response; Clustering Analysis; Immune Dysregulation

1. INTRODUCTION

Major depressive disorder (MDD) is a highly prevalent psychiatric condition and a leading cause of disability worldwide (World Health Organization, 2017). Diagnostic frameworks such as the DSM-5 define depression based on symptom severity, reflecting its association with functional impairment and healthcare burden (Beiser et al., 2019; Chen and Lin, 2011; Voelker et al., 2021; Zimmerman et al., 2018). However, growing evidence underscores the marked biological heterogeneity underlying this syndrome (Dinga et al., 2019; Drysdale et al., 2017).

In particular, a distinct immuno-inflammatory subtype of MDD has been described (Raison and Miller, 2011; Schmidt et al., 2016; Strawbridge et al., 2019). This subtype is characterized by low-grade systemic inflammation and elevated levels of C-reactive protein (CRP) and pro-inflammatory cytokines (e.g., IL-6, IL-1β, TNF-α), which have been associated with greater disorder severity (Gavril et al., 2024; Jeenger et al., 2017; Köhler-Forsberg et al., 2017; Orsolini et al., 2022; Osimo et al., 2019; Paganin and Signorini, 2024) and poorer treatment outcomes (Benedetti et al., 2021; Breit et al., 2023; Strawbridge et al., 2015), especially to antidepressants (Dahl et al., 2014; Liu et al., 2020; Uher et al., 2014; Yang et al., 2019).

Next to conventional pharmacotherapy and the gold-standard electroconvulsive therapy (ECT), repetitive transcranial magnetic stimulation (rTMS) has emerged as an effective, non-invasive neuromodulation treatment for patients with MDD, offering fewer side effects and improved tolerability. Among its protocols, intermittent theta burst stimulation (iTBS) has gained prominence due to its shorter session duration and comparable efficacy to conventional 10 Hz stimulation applied to the left dorsolateral prefrontal cortex (DLPFC) (Blumberger et al., 2018; Cole et al., 2022; Lee et al., 2023; Neuteboom et al., 2023). Nevertheless, response to iTBS remains highly variable (Kishi et al., 2024), underscoring the need for biomarkers that can predict and optimize treatment outcomes (Breit et al., 2023). Neuroinflammatory processes are increasingly recognized as modulators of synaptic plasticity and cortical excitability (Guo et al., 2023). Synaptic plasticity refers to the brain's ability to strengthen or weaken synaptic connections, whereas cortical excitability refers to the responsiveness of neurons to stimulation (Guo et al., 2023; Lenz et al., 2021). These effects are thought to involve activation of inflammatory signaling cascades such as the Janus kinase/signal transducer and activator of transcription (JAK/STAT) and nuclear factor kappa-light-chain-enhancer of activated B cells (NF-κB) pathways. These pathways regulate cytokine signaling, glial cell reactivity, and neuroplastic processes implicated in depression (Feng et al., 2024; Kennedy and Silver, 2016; Miller and Raison, 2016). This has led to the hypothesis that peripheral inflammatory activity may influence the effectiveness of iTBS treatment. However, most neuromodulation studies have examined a narrow subset of cytokines, often yielding inconsistent results (Pedraz-Petrozzi et al., 2024). A more comprehensive characterization of inflammatory profiles at the systems level (i.e.,

considering multiple interacting pathways) may therefore clarify these inconsistencies and enable more precise, biomarker-guided stratification of treatment responses.

Recent advances in high-throughput proteomic technologies, such as the Olink platform, enable the simultaneous quantification of over 90 immune-related proteins with high sensitivity and reproducibility from small plasma volumes (Assarsson et al., 2014). These approaches enable the characterization of complex, pathway-level immune signatures, moving beyond single-marker associations toward biologically grounded 'immune biotypes' - that is, distinct patient subgroups defined by shared patterns of immune activity. By providing a systems-level view of inflammatory signaling, proteomic profiling can identify patient subgroups with underlying biological differences that are not apparent from conventional clinical classifications (Fillman et al., 2014; Mesleh et al., 2021; Steiner et al., 2017; Yang et al., 2023).

In this exploratory study, we used targeted inflammatory proteomics to determine whether distinct baseline immune signatures could distinguish subgroups of patients with moderate-to-severe depression (defined by baseline MADRS ≥20) undergoing iTBS based on treatment response. By applying data-driven clustering to the Olink proteomic data, we aimed to identify inflammatory profiles based on biological markers, thereby better understanding the mechanisms underlying variability in neuromodulation outcomes. This approach aligns with the broader goal of precision psychiatry, which seeks to move beyond symptom-based classification toward biologically informed patient stratification.

2. MATERIALS AND METHODS

2.1. Study design

This exploratory analysis draws on data from a larger clinical trial that investigated the imaging, psychometric, and neuromodulatory effects of iTBS in patients with MDD (Pre-mapping Networks for Brain Stimulation 2; clinicaltrials.gov/show/NCT05260086). The main study followed a six-week longitudinal design, which has been described previously (Wilkening et al., 2022).

The trial used a quadruple-blinded, randomized, sham-controlled, crossover design, ensuring that participants, care providers, investigators, and outcome raters were unaware of treatment allocation. Each participant completed two one-week stimulation phases (one with active iTBS and one with sham stimulation). The order of these phases (active-sham or sham-active) was randomized for each participant using pre-coded sequences generated in MATLAB (The MathWorks, Inc., Natick, MA, USA). The principal investigator supervised the study while maintaining blinding from all participant interactions (Wilkening et al., 2022; Wilkening and Goya-Maldonado, 2025).

Additionally, a parallel pseudorandomized design was implemented to assess the clinical utility of personalized stimulation targeting. Participants either received stimulation at the standard F3 scalp location (following the international 10–20 EEG system) or at an individually selected site within the left DLPFC, identified via resting-state functional MRI. For this analysis, we did not differentiate between fixed and individualized targeting, as both approaches employed similar methods (Wilkening et al., 2022; Wilkening and Goya-Maldonado, 2025). Previous analyses of this cohort found no significant difference in treatment outcomes based on stimulation target group (Wilkening et al., 2025a); therefore, the entire sample was combined for the present study.

Depressive symptoms were evaluated using the Montgomery-Åsberg Depression Rating Scale (MADRS), administered by trained clinicians at baseline and again at the end of each week, allowing for the assessment of symptom changes over the six-week study period (Wilkening et al., 2022; Wilkening and Goya-Maldonado, 2025).

2.2. Participants

The study protocol complied with the Declaration of Helsinki and received approval from the Ethics Committee at the University Medical Center Göttingen (UMG). Before taking part, all participants provided both verbal and written informed consent after receiving thorough information about the study procedures (Wilkening and Goya-Maldonado, 2025). Participants were eligible if they were adults aged 18 to 60 years, met DSM-5 criteria for major depressive disorder (MDD), and were experiencing a moderate-to-severe depressive episode. Only those with a baseline MADRS score of 20 or higher were included in this exploratory study.

Trained psychiatrists confirmed MDD diagnoses using the Structured Clinical Interview for DSM-5 Disorders, Clinical Version (SCID-5-CV), and determined depression severity with the MADRS (Hengartner et al., 2020; Montgomery and Åsberg, 1979; Wilkening and Goya-Maldonado, 2025).

Exclusion criteria covered any conditions that would contraindicate rTMS, such as a history of epilepsy, significant neurological disorders, pregnancy, or the presence of metallic implants (Wilkening and Goya-Maldonado, 2025).

Participants with evidence of acute or systemic inflammation based on baseline C-reactive protein (CRP) or white blood cell count (WBC) were excluded. Specifically, individuals were excluded if CRP exceeded 10 mg/L or if the WBC was greater than 11,000 cells/μL, as these thresholds are commonly used to indicate more overt acute inflammatory or infectious processes (Gabay and Kushner, 1999; Haburchak and Alchreiki, 2020; Mank et al., 2025; Myers et al., 2004; Nehring et al., 2025). To maintain consistency, participants who used pharmacotherapy were required not to have any changes for at least two weeks prior to the study enrollment and throughout its duration. Concomitant medication was categorized for analysis as no medication at all, non-antidepressant medication, other antidepressants (non-SSRIs), and SSRIs. Antidepressants represented in the sample included SSRIs (e.g., escitalopram, sertraline, and citalopram) and non-SSRI antidepressants (e.g., venlafaxine, bupropion, duloxetine, mirtazapine, agomelatine, trazodone, and moclobemide). Frequent monitoring of serum medication levels ensured treatment adherence, and these values were incorporated into the statistical analyses to control for confounding effects on clinical outcomes (Wilkening and Goya-Maldonado, 2025). Both inpatients and outpatients were included in the sample, but all neuromodulation sessions were conducted in an outpatient setting. Details regarding study procedures and the underlying rationale have been published previously (Wilkening et al., 2022; Wilkening and Goya-Maldonado, 2025).

2.3. iTBS treatment

The technical specifications and details of the iTBS protocol applied in this study are available in the published study protocol (Wilkening et al., 2022; Wilkening and Goya-Maldonado, 2025). Briefly, the iTBS was administered using a MagVenture system equipped with MagOption and a figure-of-eight MCF-B65 A/P cooled coil, operated by trained clinical staff. Stimulation consisted of four sessions per day, each lasting approximately 10 minutes, with at least 20-minute intervals between sessions in accordance with established practices to allow for inter-session spacing (Tse et al., 2018; Wilkening and Goya-Maldonado, 2025). The iTBS paradigm involved bursts of three pulses at 50 Hz delivered at 5 Hz, with 2-second trains and 8-second rest periods. Each session comprised 60 bursts (a total of 1,800 pulses per session), amounting to 7,200 pulses per day and a cumulative 36,000 pulses during the entire treatment period.

We determined the resting motor threshold (RMT) daily using electromyography from the right first dorsal interosseous muscle. RMT was defined as the lowest intensity that evoked motor potentials of ≥50 µV in at least 5 out of 10 consecutive trials. Stimulation intensity was set at 110% of the individual RMT. For sham stimulation, we rotated the coil 180 degrees to simulate the sound associated with active stimulation while reducing the actual effective output. To further mimic the somatosensory aspects, we applied transcutaneous electrical nerve stimulation (tENS) electrodes to the scalp during both real and sham conditions. To evaluate the integrity of the blinding procedure, participants rated their experience using a visual analogue scale (Wilkening and Goya-Maldonado, 2025).

2.4. Proteomics: Inflammatory Marker Assessment and Enrichment Analysis

Peripheral venous blood samples were collected at the start of the study in tubes containing ethylenediaminetetraacetic acid (EDTA). These initial samples were drawn before group assignment (whether active-sham or sham-active). Plasma was isolated by spinning the tubes at 3,000 rpm for 15 minutes and then stored at –80°C in the university's research facilities until needed for analysis.

To measure markers of inflammation, we used the Olink® Target 96 Inflammation panel (Olink Proteomics, Uppsala, Sweden). This panel quantifies 92 inflammation-related proteins using proximity extension assay (PEA) technology. Each protein measurement is obtained using a specific pair of oligonucleotide-tagged antibodies. Once both antibodies bind to the target protein, the DNA strands are brought together, allowing them to hybridize and be amplified by real-time PCR. Data are presented as Normalized Protein Expression (NPX) values, which are $\log_2$-transformed relative units standardized by the manufacturer (Assarsson et al., 2014; Yang et al., 2023). All Olink assays took place at the Fraunhofer Institute for Translational Medicine and Pharmacology in Frankfurt am Main, Germany.

Before conducting the analyses, we assessed the quality of the NPX data. All 92 inflammatory proteins measured by the Olink® panel were present. The majority showed excellent detectability, with 82 of 92 proteins having more than 95% of NPX values above the limit of detection (LOD), and a median missingness of 0%. Overall missingness averaged ~15%, but this was almost entirely attributable to 10 low-abundance proteins with high proportions of LOD-flagged values (β-NGF, IL-2, IL-2RB, IL-20, IL-13, IL-33, LIF, IL-1α, NRTN, TSLP). Importantly, in the Olink system, values below the LOD are still provided as NPX measurements and flagged with LOD indicators rather than being removed or coded as missing (Bevital AS, 2023; Pramod Shinde, 2021). Because these <LOD values remain in the dataset, no actual data loss occurs, and no exclusion based on missingness was required; all 92 proteins were therefore retained for analysis. We also did not apply any imputation procedures (e.g., LOD substitution, mean imputation, or regression-based estimation). Given the relatively small sample size, imputation could artificially reduce variability or introduce spurious associations. Consistent with

recent recommendations suggesting that avoiding imputation can yield more robust results in smaller proteomic datasets (Bramer et al., 2021), all NPX values (including those flagged as <LOD) were analyzed as provided (Bevital AS, 2023; Pramod Shinde, 2021). This approach avoids distorting the natural biological variation that may occur when few inflammatory markers fall below the detection range in specific subgroups.

2.5. Statistical analysis

Initially, to identify potential subgroups based on baseline inflammatory marker expression, we conducted a k-means cluster analysis. Before clustering, all NPX values were standardized so that each of the 92 proteins would contribute equally, correcting for differences in scale. K-means clustering was performed on the standardized NPX values of all 92 inflammatory proteins from the Olink panel for each participant, such that each protein contributed equally after correction for differences in scale. No feature selection was performed before clustering. The Hartigan–Wong algorithm was employed for clustering, with a maximum of 1,000 iterations to ensure convergence.

To determine the optimal number of clusters, we used the Elbow method, Gap Statistics, and the average silhouette width, all applied to the standardized biomarker data. These methods consistently indicated that two clusters were optimal (see **Supplementary Material 1**). **Figure 1a** provides a graphical representation of the distributions of inflammatory markers by cluster.

We evaluated the stability and robustness of the two-cluster solution using bootstrap resampling (1,000 iterations) with the clusterboot() function (Fehrer et al., 2025; Hennig, 2024, 2007). In this analysis, the clustering algorithm was repeatedly applied to bootstrap samples of the dataset, and the cluster consistency across resamples was assessed using the Jaccard similarity coefficient. According to established benchmarks (Fehrer et al., 2025; Hennig, 2024, 2007), Jaccard values above 0.85 indicate high stability, while values below 0.50 signal cluster dissolution (Fehrer et al., 2025; Hennig, 2024, 2007). The two clusters yielded Jaccard indices of 0.955 and 0.951, showing high stability and reproducibility; none were dissolved. By contrast, cluster configurations with $k = 5$ or $k = 10$ generated fragmented clusters with lower stability (multiple Jaccard < 0.50). These findings indicate that a two-cluster solution captures the most reproducible and biologically relevant heterogeneity in our study population while minimizing the risk of overfitting.

After defining the cluster structure, we characterized the resulting groups in terms of demographic (age, sex), anthropometric (body mass index), and treatment-related variables (medication class, treatment resistance, randomization arm), as well as change in depressive symptoms. Changes in the MADRS total score (ΔMADRS = post-treatment MADRS minus baseline MADRS) were compared between clusters using t-tests. This allowed examination of potential differences in treatment outcomes between the subgroups. Categorical variables, such as sex, medication class, baseline treatment resistance, randomization group, and responder rates (defined as ≥ 50% reduction in

MADRS total score), were analyzed by chi-square tests. Symptom-level differences within the two-cluster solution were explored descriptively with radar plots showing changes in individual MADRS items from baseline to post-treatment across clusters. To assess whether concomitant medication might confound the association between inflammatory cluster membership and treatment response, we performed sensitivity analyses including medication category, medication-free status, and baseline medication load. Concerning the latter, to account for the psychotropic medication load, following our previous publication (Wilkening et al., 2025b), we summed for each individual the estimated intake dose of each substance at baseline, based on the interview or, when possible, on the circulating blood levels (below = 1, normal = 2, or above = 3 of the expected doses for each medication). Because some medication subgroups were small, adjusted responder models were estimated using Firth penalized logistic regression.

We next performed differential expression analyses for the inflammatory proteins. For each protein, we calculated mean NPX differences between clusters and used Welch's t-tests for statistical comparison. Volcano plots display the relationship between $\log_2$ NPX differences and significance. To correct for multiple testing, we applied the Benjamini-Hochberg FDR method. Proteins were considered significantly differentially expressed if $|\Delta NPX| > 1$ (about a two-fold change on the $\log_2$ scale) and Benjamini-Hochberg adjusted p-value < 0.05, in line with recent recommendations in Olink-based studies (Fredolini et al., 2024; Tayal et al., 2022; Wen et al., 2025). This threshold exceeds expected technical variation, helping to prioritize robust, biologically meaningful effects. Standardized effect sizes, such as Cohen's d, Hedges' g (for small sample correction), and Glass's Δ (for variance differences), were calculated for each significant protein to quantify between-group differences.

In the final step, we analyzed pathways to provide a biological context for our results. Proteins exhibiting significant expression differences between clusters were subjected to pathway enrichment analysis using the Kyoto Encyclopedia of Genes and Genomes (KEGG) and Reactome databases. This allowed us to identify biological and signaling processes associated with proteins whose expression varied between clusters. Enrichment results are presented with q-values and false discovery rates (FDR), with statistical significance defined as $q < 0.05$ and $FDR < 0.05$.

All statistics and visualizations, including enrichment analyses, were performed in RStudio (version 2024.12.1+563).

3. RESULTS

3.1. *Subgroup characterization: general characteristics, clinical outcomes and symptom interaction*.

The sample comprised 54 participants, with 28 assigned to Cluster 1 and 26 to Cluster 2 (**Table 1)**. The two clusters did not differ significantly in demographic or baseline clinical characteristics, including age, sex, BMI, treatment resistance, medication class, or randomization order (all $p > 0.12$; **Table 1**). With regard to treatment outcome, Cluster 2 showed a significantly higher proportion of responders than Cluster 1 ($p = 0.031$; **Table 1**; **Figure 1b**). By contrast, baseline MADRS scores and mean change in total MADRS score did not differ significantly between clusters (**Table 1**; **Figure 1c**). Thus, although the mean reduction in total MADRS score was comparable across groups, a larger proportion of patients in Cluster 2 achieved clinically meaningful symptom relief, defined as a reduction of at least 50% in MADRS total score. This suggests that baseline inflammatory differences may be more closely related to the likelihood of achieving a categorical response than to average symptom change.

Exploratory analysis of symptom-level changes (ΔMADRS items) revealed broadly similar improvement patterns across clusters, with reductions observed across all MADRS items (**Table 1**; **Figure 1d**). Descriptively, Cluster 2 showed greater improvement across several symptom domains, particularly reduced sleep, lassitude, inability to feel, and suicidal thoughts. However, these item-level differences were exploratory and descriptive, were not formally tested statistically, and should therefore be interpreted with caution.

3.2. Sensitivity analysis for medication-related confounding

To assess whether medication use alone might explain the association between inflammatory cluster membership and treatment response, we performed additional sensitivity analyses. Medication category was not significantly associated with cluster assignment (Chi-square test: $\chi^2(3) = 0.60$, $p = 0.897$) or responder status (Chi-square test: $\chi^2(3) = 3.11$, $p = 0.375$). Likewise, baseline medication load did not differ significantly by cluster or responder status (all $p > 0.59$). Because some medication subgroups were small, adjusted responder models were estimated using Firth penalized logistic regression. In these analyses, cluster membership remained significantly associated with treatment response after adjustment for medication category (OR = 3.64, 95% CI 1.21–11.83, $p = 0.021$), baseline medication load (OR = 3.19, 95% CI 1.09–9.90, $p = 0.034$), and simplified medication status (medication-free vs. medicated; OR = 3.30, 95% CI 1.11–10.48, $p = 0.031$). Full results are provided in Supplementary Material 1.

3.3. Inflammatory parameters - differences between Cluster 1 and 2

After identifying significant differences in symptom alleviation between Clusters 1 and 2, we examined their inflammatory marker profiles, as these clusters represented opposite

extremes: Cluster 2 included the highest proportion of treatment responders, whereas Cluster 1 contained the fewest.

To visualize and quantify molecular differences, we generated a volcano plot based on NPX values, with p-values adjusted for multiple comparisons using the Benjamini–Hochberg FDR procedure. Markers were considered significant when both criteria were met: FDR < 0.05 and an absolute NPX difference ≥ 1 ($\log_2$ scale). Of the 92 inflammatory proteins analyzed, 47 showed FDR-adjusted $p < 0.05$ (including MCP-4, CXCL6, CXCL5, IL-8, IL-7, VEGFA, CXCL1, MCP-1, CXCL11, OSM, MMP-1, HGF, CCL4, LAP TGF-β1, CD40, β-NGF, TNFSF14, CCL11, CSF1, MCP-2, LIFR, CCL28, FGF5, IL-2, AXIN1, TWEAK, TGF-α, FGF23, IL-6, MCP-3, CXCL10, IL-18, CD244, TSLP, CD8A, CCL3, IL10RB, IL20, LIF, SCF, IL15RA, CX3CL1, TNF, OPG, IL24, CCL23, and CCL25; **Supplementary Material 2**). However, only ten proteins satisfied both significance thresholds (FDR < 0.05 and |ΔNPX| ≥ 1), specifically MCP-4, CXCL6, IL-7, TNFSF14, CXCL1, OSM, CXCL5, IL-8, CXCL11, and MMP-1. We applied the additional |ΔNPX| ≥ 1 threshold to prioritize proteins that were not only statistically significant, but also associated with larger effect sizes. This criterion further emphasized differences likely to be biologically meaningful and greater than the expected technical variability of the assay. These outcomes are shown in the volcano plot (**Figure 2**) and the corresponding boxplots (**Figure 3**), which illustrate the expression differences between Clusters 1 and 2.

The |ΔNPX| ≥ 1.0 criterion ensured that only proteins showing at least a two-fold relative difference between clusters were included, emphasizing changes that are likely to be biologically relevant and greater than the expected technical variability of the assay. To provide a more comprehensive assessment of these differences, p-values were supplemented with standardized effect-size metrics for all pairwise cluster comparisons, with particular attention to Clusters 1 and 2, where the greatest disparities were observed. In these analyses, Cohen's d (with 95% confidence intervals), Hedges' g (corrected for small sample bias), and Glass's Δ (adjusting for unequal variances) were computed for each relevant protein. Across these metrics, the key proteins differentiating the clusters demonstrated consistently large effect sizes (e.g., MCP4: Cohen's d = 3.18, Hedges' g = 3.13; IL7: Cohen's d = 2.40, Hedges' g = 2.36; **Supplementary Material 1**). These results collectively reveal strong and biologically significant differences between clusters, even given the relatively small subgroup sizes. Furthermore, all proteins that met the significance criteria were quantifiable for all participants above the detection limit (see Methods).

3.4. Enrichment analysis:

To explore the biological significance of the baseline differentially expressed proteins between clusters, we performed KEGG pathway enrichment analysis using the full inflammatory proteome as background. Several immune and inflammatory pathways were significantly enriched (**Figure 4a**). The most prominent pathway was cytokine–cytokine receptor interaction (FDR = 9.94×10^{-12}; q = 5.37×10^{-12}), highlighting broad

involvement of intercellular signaling mechanisms that regulate immune activation. Additional enriched pathways included viral protein interaction with cytokine and cytokine receptor (FDR = 2.65×10^{-11}; q = 1.43×10^{-11}), chemokine signaling (FDR = 1.66×10^{-7}; q = 8.98×10^{-8}), and IL-17 signaling (FDR = 1.70×10^{-7}; q = 9.19×10^{-8}), all of which are closely associated with pro-inflammatory cytokine cascades. Pathways linked to rheumatoid arthritis (FDR = 1.70×10^{-7}; q = 9.19×10^{-8}) and NF-κB signaling (FDR = 1.83×10^{-5}; q = 9.88×10^{-6}) further indicate activation of canonical immune processes. Other relevant pathways, including TNF signaling, Toll-like receptor signaling, and JAK–STAT signaling, were also enriched, reinforcing the role of inflammatory signal transduction in these proteomic differences. A complete list of enriched KEGG pathways is provided in **Supplementary Material 1**.

Reactome pathway enrichment analysis was conducted to identify biological processes associated with the differentially expressed proteins between clusters. The analysis revealed significant enrichment of pathways primarily related to chemokine and cytokine receptor signaling and G protein–coupled receptor (GPCR)–mediated signaling (**Figure 4b**). The most significantly enriched pathway was "Chemokine receptors bind chemokines" (FDR = 9.11×10^{-11}; q = 3.55×10^{-11}), involving six of the ten proteins identified. Similarly, "Peptide ligand-binding receptors" (FDR = 8.22×10^{-8}; q = 3.21×10^{-8}), "G alpha (i) signaling events" (FDR = 8.52×10^{-7}; q = 3.32×10^{-7}), and "Class A/1 (Rhodopsin-like) receptors" (FDR = 8.56×10^{-7}; q = 3.34×10^{-7}) were among the top enriched pathways, underscoring a strong contribution of GPCR signaling. Downstream cytokine signaling cascades were also significantly enriched, including "Signaling by interleukins" (FDR = 1.09×10^{-4}; q = 4.23×10^{-5}), "Interleukin-4 and Interleukin-13 signaling" (FDR = 3.83×10^{-4}; q = 1.49×10^{-4}), and "Interleukin-10 signaling" (FDR = 2.56×10^{-3}; q = 9.96×10^{-4}). Additional pathways related to TNF receptor signaling, IL-6–type cytokine receptor interactions, and ATF4-mediated stress response were also identified at nominal significance levels. Complete Reactome enrichment results are provided in **Supplementary Material 1**.

4. DISCUSSION

Our findings demonstrate that patients with moderate-to-severe depression undergoing iTBS can be stratified into subgroups according to baseline inflammatory proteomic profiles, which are related with differences in treatment response. This extends prior evidence of biological heterogeneity in MDD observed in proteomic and multimodal studies (Milaneschi et al., 2020; Tang et al., 2025) and immune profiling (Hagenberg et al., 2025) by linking inflammation directly to neuromodulation outcomes. Two molecular phenotypes were identified, differing significantly in iTBS response but not in demographic or clinical confounders, suggesting that the variability may be related to immunological factors. Cluster 2 exhibited the highest response rate, whereas Cluster 1 contained the most non-responders, suggesting that baseline immune tone may be associated with therapeutic efficacy. Notably, the two clusters did not differ in baseline symptom severity or in mean change in total MADRS score. The principal clinical difference therefore lay in the likelihood of achieving a categorical treatment response rather than in average MADRS symptom reduction. When examining individual MADRS items descriptively, Cluster 2 also showed a tendency toward broader symptom improvement across several domains.

These findings support the view that MDD encompasses biologically (and to some extent, immunologically) distinct subtypes, one characterized by immune activation that may interfere with treatment response. While most depressed patients exhibit cytokine levels within the normal range, a substantial subset (estimated at one third) shows a pro-inflammatory phenotype (Miller and Raison, 2016; Osimo et al., 2019; Schmidt et al., 2016) linked to poorer antidepressant outcomes (Gadad et al., 2017; O'Brien et al., 2007; Strawbridge et al., 2015; Uher et al., 2014). The present findings indicate that such immune heterogeneity may similarly modulate response to iTBS, extending the relevance of inflammation beyond pharmacological treatment resistance.

Inflammatory cytokines appear to influence not only the onset and progression of depression but also responsiveness to treatment. Patients who respond to antidepressants typically exhibit normalization of cytokine levels, whereas non-responders maintain or increase inflammatory activity during therapy (Syed et al., 2018; Yilmaz et al., 2022). Elevated baseline IL-6, IL-8, and TNF-α have been consistently associated with reduced antidepressant efficacy (Gadad et al., 2017; Liu et al., 2020; Uher et al., 2014). Mechanistically, inflammation can also directly influence neural processes relevant to the antidepressant effects of iTBS. Pro-inflammatory cytokines such as IL-6, IL-8, and TNF-α, frequently elevated in patients with major depressive disorder (Krsek et al., 2024), are known to modulate synaptic plasticity (Lisowska, 2025; Singhal and Baune, 2017; Yirmiya and Goshen, 2011), processes critical for neuromodulation efficacy. Furthermore, TNF-α, IL-8, IFN-γ, and activation of the kynurenine pathway have been associated with alterations in white-matter microstructure in mood disorders (Poletti et al., 2024), suggesting that inflammatory

dysregulation may extend beyond local synaptic effects to impact large-scale neural network integrity. Matrix metalloproteinases (e.g. MMP-1, which was elevated in the least responsive cluster) play dual roles in the central nervous system, mediating extracellular matrix remodeling essential for synaptic plasticity while, when dysregulated, contributing to blood–brain barrier breakdown and neuroinflammatory propagation (Hassamal, 2023; Huntley, 2012). Dysregulation of MMP signaling can therefore alter the neuronal microenvironment and limit synaptic remodeling, potentially reducing responsiveness to plasticity-inducing interventions (Alaiyed and Conant, 2019; Beroun et al., 2019).

Although our study assessed peripheral inflammatory proteins rather than direct central markers, peripheral immune activation can influence neuroinflammatory processes through several pathways, including cytokine signaling across the blood–brain barrier, endothelial and glial activation, and downstream effects on microglial function and kynurenine metabolism. In depression, such neuroimmune signaling has been linked to altered synaptic plasticity, impaired neurotrophic support, and disrupted network-level brain function, all of which are relevant to the proposed mechanism of iTBS. Preclinical studies further support this relationship by showing that depression-like behavior can be ameliorated through interventions that reduce neuroinflammation and related oxidative or nitrosative stress (Qiu et al., 2020; Ye et al., 2024).

From this perspective, the inflammatory profiles identified here may reflect not only systemic immune tone but also peripheral correlates of neuroinflammatory states that could reduce responsiveness to neuromodulation. Consistent with this interpretation, translational evidence indicates that heightened systemic inflammation is associated with diminished therapeutic responsiveness (Haroon et al., 2018), and reviews of rTMS in depression suggest that immune-inflammatory markers may be linked to neuromodulatory outcome (Rajkumar, 2023). Conversely, neuromodulation itself appears to exert immunoregulatory effects, reducing circulating pro-inflammatory cytokines and normalizing plasma MMP concentrations (Cirillo et al., 2023; Wang et al., 2022). In summary, these findings support the idea that iTBS may engage neuroimmune mechanisms and that specific inflammatory states could interfere with cortical plasticity and thereby attenuate treatment response.

The specific proteins that distinguish the poorer-outcome Cluster 1 provide further insight into the potential mechanisms underlying differential response to iTBS. The ten proteins that distinguish the two inflammatory clusters (MCP-4, CXCL6, IL-7, CXCL1, OSM, CXCL5, IL-8, TNFSF14, CXCL11, and MMP-1) are associated with enhanced chemotaxis, cytokine signaling, and extracellular matrix remodeling. These proteins are involved in immune pathways governing leukocyte recruitment and cytokine–cytokine receptor interactions, suggesting that non-responders may have a more pro-inflammatory profile. Consistent with this, enrichment analyses identified three major pathways with the strongest statistical support: cytokine–cytokine receptor interaction, chemokine receptor binding chemokines, and G-protein–coupled receptor (GPCR)

signaling events. Together, these networks regulate immune cell trafficking, receptor-mediated signaling, and cellular responses to inflammatory stress. IL-8, a potent chemoattractant that drives neutrophil migration (Yoshimura et al., 1987), and related CXC chemokines (CXCL1, CXCL5, CXCL6, CXCL11) orchestrate leukocyte recruitment in the central nervous system (Milenkovic et al., 2019; Stuart et al., 2015) and have been linked to increased neuroinflammation and reduced antidepressant efficacy (Gasparini et al., 2022; Liu et al., 2020). MCP-4, a member of the MCP1–5 family, enhances macrophage chemotaxis and promotes chronic immune activation (Stuart et al., 2015). Oncostatin M (OSM), a pleiotropic IL-6–family cytokine, promotes endothelial activation and leukocyte transmigration (Han et al., 2023; Modur et al., 1997) and has been implicated in pro-inflammatory and mood-related signaling cascades (Franzen et al., 2020; Knight, 2022; Richards, 2013; Tanaka and Miyajima, 2003). IL-7, which regulates T-cell proliferation and survival (Chen et al., 2021), may further modulate neuroimmune crosstalk, while MMP-1, a matrix metalloproteinase central to extracellular matrix remodeling (Pardo and Selman, 2005), can affect synaptic integrity and blood–brain-barrier permeability when dysregulated (Hassamal, 2023; Huntley, 2012). Collectively, these findings suggest that upregulated cytokine and chemokine signaling, coupled with aberrant matrix remodeling, may be associated with lower iTBS efficacy, whereas lower inflammatory tone may be associated with better response.

The principal strength of this study lies in its data-driven identification of inflammatory subgroups in moderate-to-severe depression, linking baseline immune profiles to differential iTBS outcomes and enrichment of cytokine and interleukin signaling pathways. However, several limitations must be considered. The exploratory design precludes causal inference, and findings should be regarded as hypothesis-generating pending replication in larger, longitudinal cohorts. In particular, the relatively small number of participants within each cluster (Cluster 1: n = 28; Cluster 2: n = 26) limits statistical precision and calls for cautious interpretation of subgroup estimates, even though the clustering solution itself showed high bootstrap stability. Analyses were restricted to baseline protein expression; inclusion of post-treatment data would clarify how inflammatory signatures evolve with iTBS. Additionally, the lack of comparator arms (e.g., pharmacotherapy or ECT) constrains conclusions about the specificity of these immune patterns to neuromodulation. While the Olink® Inflammation panel focuses on inflammation-related proteins, which aligns well with our a priori interest based on previous findings, future work using broader proteomic approaches may help to uncover additional biological pathways associated with iTBS outcomes and treatment response. Furthermore, the modest number of significant proteins and the presence of potential confounders (such as lifestyle and psychosocial factors) further limit interpretability. Although participants differed in concomitant medication, sensitivity analyses suggested that neither medication category nor medication load explained the observed association between inflammatory cluster membership and treatment response. Finally, since all participants presented with moderate-to-severe depression, the

generalizability of these findings to milder forms of depression remains uncertain. Nevertheless, using a conservative $|\Delta NPX| \geq 1$ threshold (≈2-fold change on the $\log_2$ scale) ensured robust, interpretable results, and all significant proteins achieved power > 0.99 (**see Supplementary Material 1**).

In conclusion, baseline inflammatory proteomic profiles are associated with subgroups of patients with moderate-to-severe depression who differ in their clinical response to iTBS. Cluster 1, defined by elevated cytokine- and chemokine-related markers, showed poorer outcomes, whereas Cluster 2, characterized by lower baseline immune activity, exhibited better improvement. Cytokine signaling pathways regulate proliferation, apoptosis, and immune activation (Voßhenrich and Santo, 2002), and excessive activation has been associated with reduced cortical adaptability. These findings support the concept that immune dysregulation contributes to treatment resistance and may serve as a biological modifier of neuromodulatory efficacy. Future research should validate these results in larger cohorts, incorporate post-treatment proteomics and neuroimaging, and test whether the ten significant markers predict responsiveness across treatment modalities. Ultimately, such research could guide precision-based interventions, including anti-inflammatory augmentation strategies, for patients with depression who exhibit an inflammatory profile.

5. ACKNOWLEGEMENTS

This work was supported by the German Federal Ministry of Education and Research (*Bundesministerium für Bildung und Forschung, BMBF: 01 ZX 1507*, ‘‘PreNeSt - e:Med’’) and the to the foundation *Immunität und Seele (https://immunitaet-und-seele.de/)*. The authors thank the team of Dr. Nicole Ziegler (Fraunhofer Institute for Translational Medicine and Pharmacology, Frankfurt am Main, Germany) for their assistance in analyzing blood samples using proteomics panels.

6. CONFLICTS OF INTEREST AND OTHER STATEMENTS

Ethics Approval and Consent to Participate: The study protocol was conducted in accordance with the Declaration of Helsinki and was approved by the Ethics Committee of the University Medical Center Göttingen (UMG). All participants provided both verbal and written informed consent after receiving a full explanation of the study procedures.

Consent for Publication: Not applicable.

Availability of Data and Materials: The data supporting the findings of this study are not publicly available due to European Union data protection regulations. However, data may be made available upon reasonable request from the corresponding author, provided appropriate legal and ethical conditions are met.

Statement: During the preparation of this manuscript, the authors used Grammarly Inc., Nature Research Assistant, and ChatGPT to assist with language refinement and grammar correction. Elicit was used to support the literature search. All content was critically reviewed and edited by the authors, who take full responsibility for the final version of the manuscript.

Competing Interests: The authors declare that they have no competing interests.

Funding: This project received financial support from the German Federal Ministry of Education and Research (*Bundesministerium für Bildung und Forschung, BMBF: 01 ZX 1507*, ‘‘PreNeSt - e:Med’’) and the foundation *Immunität und Seele* (Prof. Dr. Norbert Müller *https://immunitaet-und-seele.de/*). The funders had no role in the study design, data collection, analysis, interpretation, or manuscript preparation.

Employment: None of the authors was employed or contracted by any organization that could gain or lose financially from the publication of this manuscript.

Personal Financial Interests: The authors did not receive any form of financial compensation (e.g., salaries, stocks, consulting fees) from commercial entities related to this research.

Declarations of Interest: Bruno Pedraz acknowledges receiving a Seed Money for Research grant from the Central Institute of Mental Health and receiving a grant from the foundation *Immunität und Seele*. Roberto Goya-Maldonado acknowledges receiving a grant from the German Federal Ministry of Education and Research (*Bundesministerium für Bildung und Forschung, BMBF: 01 ZX 1507*, ‘‘PreNeSt-e:Med’’).

7. REFERENCES

Alaiyed, S., Conant, K., 2019. A Role for Matrix Metalloproteases in Antidepressant Efficacy. Front. Mol. Neurosci. 12. https://doi.org/10.3389/fnmol.2019.00117

Assarsson, E., Lundberg, M., Holmquist, G., et al., 2014. Homogenous 96-Plex PEA Immunoassay Exhibiting High Sensitivity, Specificity, and Excellent Scalability. PLOS ONE 9, e95192. https://doi.org/10.1371/journal.pone.0095192

Beiser, D.G., Ward, C.E., Vu, M., et al., 2019. Depression in Emergency Department Patients and Association With Health Care Utilization. Acad. Emerg. Med. 26, 878–888. https://doi.org/10.1111/acem.13726

Benedetti, F., Poletti, S., Vai, B., et al., 2021. Higher baseline interleukin-1β and TNF-α hamper antidepressant response in major depressive disorder. Eur. Neuropsychopharmacol. J. Eur. Coll. Neuropsychopharmacol. 42, 35–44. https://doi.org/10.1016/j.euroneuro.2020.11.009

Beroun, A., Mitra, S., Michaluk, P., et al., 2019. MMPs in learning and memory and neuropsychiatric disorders. Cell. Mol. Life Sci. 76, 3207–3228. https://doi.org/10.1007/s00018-019-03180-8

Bevital AS, 2023. Bevital´s Olink FAQ [WWW Document]. URL https://bevital.no/olink/ (accessed 11.13.25).

Blumberger, D.M., Vila-Rodriguez, F., Thorpe, K.E., et al., 2018. Effectiveness of theta burst versus high-frequency repetitive transcranial magnetic stimulation in patients with depression (THREE-D): a randomised non-inferiority trial. The Lancet 391, 1683–1692. https://doi.org/10.1016/S0140-6736(18)30295-2

Bramer, L.M., Irvahn, J., Piehowski, P.D., et al., 2021. A Review of Imputation Strategies for Isobaric Labeling-Based Shotgun Proteomics. J. Proteome Res. 20, 1–13. https://doi.org/10.1021/acs.jproteome.0c00123

Breit, S., Mazza, E., Poletti, S., et al., 2023. White matter integrity and pro-inflammatory cytokines as predictors of antidepressant response in MDD. J. Psychiatr. Res. 159, 22–32. https://doi.org/10.1016/j.jpsychires.2022.12.009

Chen, D., Tang, T.-X., Deng, H., et al., 2021. Interleukin-7 Biology and Its Effects on Immune Cells: Mediator of Generation, Differentiation, Survival, and Homeostasis. Front. Immunol. 12, 747324. https://doi.org/10.3389/fimmu.2021.747324

Chen, Y.-H., Lin, H.-C., 2011. Increased risk of cancer subsequent to severe depression--a nationwide population-based study. J. Affect. Disord. 131, 200–206. https://doi.org/10.1016/j.jad.2010.12.006

Cirillo, G., Pepe, R., Siciliano, M., et al., 2023. Long-Term Neuromodulatory Effects of Repetitive Transcranial Magnetic Stimulation (rTMS) on Plasmatic Matrix Metalloproteinases (MMPs) Levels and Visuospatial Abilities in Mild Cognitive Impairment (MCI). Int. J. Mol. Sci. 24. https://doi.org/10.3390/ijms24043231

Cole, E.J., Phillips, A.L., Bentzley, B.S., et al., 2022. Stanford Neuromodulation Therapy (SNT): A Double-Blind Randomized Controlled Trial. Am. J. Psychiatry 179, 132–141. https://doi.org/10.1176/appi.ajp.2021.20101429

Dahl, J., Ormstad, H., Aass, H.C.D., et al., 2014. The plasma levels of various cytokines are increased during ongoing depression and are reduced to normal levels after recovery. Psychoneuroendocrinology 45, 77–86. https://doi.org/10.1016/j.psyneuen.2014.03.019

Dinga, R., Schmaal, L., Penninx, B.W.J.H., et al., 2019. Evaluating the evidence for biotypes of depression: Methodological replication and extension of. NeuroImage Clin. 22, 101796. https://doi.org/10.1016/j.nicl.2019.101796

Drysdale, A.T., Grosenick, L., Downar, J., et al., 2017. Resting-state connectivity biomarkers define neurophysiological subtypes of depression. Nat. Med. 23, 28–38. https://doi.org/10.1038/nm.4246

Fehrer, T., Moder, L., Röglinger, M., 2025. A Taxonomy for Process Improvement and Innovation Systems. Bus. Inf. Syst. Eng. https://doi.org/10.1007/s12599-025-00928-4

Feng, X., Ma, X., Li, J., et al., 2024. Inflammatory Pathogenesis of Post-stroke Depression. Aging Dis. 16, 209–238. https://doi.org/10.14336/AD.2024.0203

Fillman, S.G., Sinclair, D., Fung, S.J., et al., 2014. Markers of inflammation and stress distinguish subsets of individuals with schizophrenia and bipolar disorder. Transl. Psychiatry 4, e365. https://doi.org/10.1038/tp.2014.8

Franzen, A.D., Lam, T.T., Williams, K.R., et al., 2020. Cerebrospinal fluid proteome evaluation in major depressive disorder by mass spectrometry. BMC Psychiatry 20, 481. https://doi.org/10.1186/s12888-020-02874-9

Fredolini, C., Dodig-Crnković, T., Bendes, A., et al., 2024. Proteome profiling of home-sampled dried blood spots reveals proteins of SARS-CoV-2 infections. Commun. Med. 4, 55. https://doi.org/10.1038/s43856-024-00480-4

Gabay, C., Kushner, I., 1999. Acute-Phase Proteins and Other Systemic Responses to Inflammation. N. Engl. J. Med. 340, 448–454. https://doi.org/10.1056/NEJM199902113400607

Gadad, B.S., Jha, M.K., Grannemann, B.D., et al., 2017. Proteomics profiling reveals inflammatory biomarkers of antidepressant treatment response: Findings from the CO-MED trial. J. Psychiatr. Res. 94, 1–6. https://doi.org/10.1016/j.jpsychires.2017.05.012

Gasparini, A., Callegari, C., Lucca, G., et al., 2022. Inflammatory Biomarker and Response to Antidepressant in Major Depressive Disorder: a Systematic Review and Meta-Analysis. Psychopharmacol. Bull. 52, 36–52.

Gavril, Radu, Dobrin, P.R., et al., 2024. Predictive Value of Inflammatory Biomarkers in Assessing Major Depression in Adults. Biomedicines 12, 2501. https://doi.org/10.3390/biomedicines12112501

Guo, B., Zhang, M., Hao, W., et al., 2023. Neuroinflammation mechanisms of neuromodulation therapies for anxiety and depression. Transl. Psychiatry 13, 1–12. https://doi.org/10.1038/s41398-022-02297-y

Haburchak, D.R., Alchreiki, M., 2020. Inpatients With “Unexplained” Leukocytosis. Am. J. Med. 133, 508–514. https://doi.org/10.1016/j.amjmed.2019.10.019

Hagenberg, J., Brückl, T.M., Erhart, M., et al., 2025. Dissecting depression symptoms: Multi-omics clustering uncovers immune-related subgroups and cell-type specific dysregulation. Brain. Behav. Immun. 123, 353–369. https://doi.org/10.1016/j.bbi.2024.09.013

Han, L., Yan, J., Li, T., et al., 2023. Multifaceted oncostatin M: novel roles and therapeutic potential of the oncostatin M signaling in rheumatoid arthritis. Front. Immunol. 14. https://doi.org/10.3389/fimmu.2023.1258765

Haroon, E., Daguanno, A.W., Woolwine, B.J., et al., 2018. Antidepressant treatment resistance is associated with increased inflammatory markers in patients with

major depressive disorder. Psychoneuroendocrinology 95, 43–49. https://doi.org/10.1016/j.psyneuen.2018.05.026
Hassamal, S., 2023. Chronic stress, neuroinflammation, and depression: an overview of pathophysiological mechanisms and emerging anti-inflammatories. Front. Psychiatry 14. https://doi.org/10.3389/fpsyt.2023.1130989
Hengartner, M.P., Jakobsen, J.C., Sørensen, A., et al., 2020. Efficacy of new-generation antidepressants assessed with the Montgomery-Asberg Depression Rating Scale, the gold standard clinician rating scale: A meta-analysis of randomised placebo-controlled trials. PLOS ONE 15, e0229381. https://doi.org/10.1371/journal.pone.0229381
Hennig, C., 2024. fpc: Flexible Procedures for Clustering.
Hennig, C., 2007. Cluster-wise assessment of cluster stability. Comput. Stat. Data Anal. 52, 258–271. https://doi.org/10.1016/j.csda.2006.11.025
Huntley, G.W., 2012. Synaptic circuit remodelling by matrix metalloproteinases in health and disease. Nat. Rev. Neurosci. 13, 743–757. https://doi.org/10.1038/nrn3320
Jeenger, J., Sharma, M., Mathur, D.M., et al., 2017. Associations of number and severity of depressive episodes with C-reactive protein and Interleukin-6. Asian J. Psychiatry 27, 71–75. https://doi.org/10.1016/j.ajp.2017.02.016
Kennedy, R.H., Silver, R., 2016. Neuroimmune Signaling: Cytokines and the CNS, in: Pfaff, D.W., Volkow, N.D. (Eds.), Neuroscience in the 21st Century. Springer, New York, NY, pp. 1–41. https://doi.org/10.1007/978-1-4614-6434-1_174-1
Kishi, T., Ikuta, T., Sakuma, K., et al., 2024. Theta burst stimulation for depression: a systematic review and network and pairwise meta-analysis. Mol. Psychiatry 29, 3893–3899. https://doi.org/10.1038/s41380-024-02630-5
Knight, D., 2022. Oncostatin M, in: Janes, S.M. (Ed.), Encyclopedia of Respiratory Medicine (Second Edition). Academic Press, Oxford, pp. 723–727. https://doi.org/10.1016/B978-0-08-102723-3.00238-9
Köhler-Forsberg, O., Buttenschøn, H.N., Tansey, K.E., et al., 2017. Association between C-reactive protein (CRP) with depression symptom severity and specific depressive symptoms in major depression. Brain. Behav. Immun. 62, 344–350. https://doi.org/10.1016/j.bbi.2017.02.020
Krsek, A., Ostojic, L., Zivalj, D., et al., 2024. Navigating the Neuroimmunomodulation Frontier: Pioneering Approaches and Promising Horizons—A Comprehensive Review. Int. J. Mol. Sci. 25. https://doi.org/10.3390/ijms25179695
Lee, N.A., Kung, S., Hu, Y., et al., 2023. Depression and anxiety outcomes of adults undergoing intermittent theta burst stimulation (iTBS) treatment for major depressive disorder: A naturalistic study. J. Mood Anxiety Disord. 3. https://doi.org/10.1016/j.xjmad.2023.100028
Lenz, M., Eichler, A., Vlachos, A., 2021. Monitoring and Modulating Inflammation-Associated Alterations in Synaptic Plasticity: Role of Brain Stimulation and the Blood-Brain Interface. Biomolecules 11, 359. https://doi.org/10.3390/biom11030359
Lisowska, K.A., 2025. The Role of Interleukin-8 (IL-8) in Treatment-Resistant Depression: A Review of Mechanisms, Biomarker Potential, and Therapeutic Implications. Int. J. Mol. Sci. 26. https://doi.org/10.3390/ijms262010092
Liu, J.J., Wei, Y.B., Strawbridge, R., et al., 2020. Peripheral cytokine levels and response to antidepressant treatment in depression: a systematic review and meta-

analysis. Mol. Psychiatry 25, 339–350. https://doi.org/10.1038/s41380-019-0474-5

Mank, V., Azhar, W., Brown, K., 2025. Leukocytosis, in: StatPearls. StatPearls Publishing, Treasure Island (FL).

Mesleh, A.G., Abdulla, S.A., El-Agnaf, O., 2021. Paving the Way toward Personalized Medicine: Current Advances and Challenges in Multi-OMICS Approach in Autism Spectrum Disorder for Biomarkers Discovery and Patient Stratification. J. Pers. Med. 11, 41. https://doi.org/10.3390/jpm11010041

Milaneschi, Y., Lamers, F., Berk, M., et al., 2020. Depression Heterogeneity and Its Biological Underpinnings: Toward Immunometabolic Depression. Biol. Psychiatry 88, 369–380. https://doi.org/10.1016/j.biopsych.2020.01.014

Milenkovic, V.M., Stanton, E.H., Nothdurfter, C., et al., 2019. The Role of Chemokines in the Pathophysiology of Major Depressive Disorder. Int. J. Mol. Sci. 20, 2283. https://doi.org/10.3390/ijms20092283

Miller, A.H., Raison, C.L., 2016. The role of inflammation in depression: from evolutionary imperative to modern treatment target. Nat. Rev. Immunol. 16, 22–34. https://doi.org/10.1038/nri.2015.5

Modur, V., Feldhaus, M.J., Weyrich, A.S., et al., 1997. Oncostatin M is a proinflammatory mediator. In vivo effects correlate with endothelial cell expression of inflammatory cytokines and adhesion molecules. J. Clin. Invest. 100, 158–168. https://doi.org/10.1172/JCI119508

Montgomery, S.A., Åsberg, M., 1979. A New Depression Scale Designed to be Sensitive to Change. Br. J. Psychiatry 134, 382–389. https://doi.org/10.1192/bjp.134.4.382

Myers, G.L., Rifai, N., Tracy, R.P., et al., 2004. CDC/AHA Workshop on Markers of Inflammation and Cardiovascular Disease: Application to Clinical and Public Health Practice: report from the laboratory science discussion group. Circulation 110, e545-549. https://doi.org/10.1161/01.CIR.0000148980.87579.5E

Nehring, S.M., Goyal, A., Patel, B.C., 2025. C Reactive Protein, in: StatPearls. StatPearls Publishing, Treasure Island (FL).

Neuteboom, D., Zantvoord, J.B., Goya-Maldonado, R., et al., 2023. Accelerated intermittent theta burst stimulation in major depressive disorder: A systematic review. Psychiatry Res. 327, 115429. https://doi.org/10.1016/j.psychres.2023.115429

O'Brien, S.M., Scully, P., Fitzgerald, P., et al., 2007. Plasma cytokine profiles in depressed patients who fail to respond to selective serotonin reuptake inhibitor therapy. J. Psychiatr. Res. 41, 326–331. https://doi.org/10.1016/j.jpsychires.2006.05.013

Orsolini, L., Pompili, S., Tempia Valenta, S., et al., 2022. C-Reactive Protein as a Biomarker for Major Depressive Disorder? Int. J. Mol. Sci. 23, 1616. https://doi.org/10.3390/ijms23031616

Osimo, E.F., Baxter, L.J., Lewis, G., et al., 2019. Prevalence of low-grade inflammation in depression: a systematic review and meta-analysis of CRP levels. Psychol. Med. 49, 1958–1970. https://doi.org/10.1017/S0033291719001454

Paganin, W., Signorini, S., 2024. Inflammatory biomarkers in depression: scoping review. BJPsych Open 10, e165. https://doi.org/10.1192/bjo.2024.787

Pardo, A., Selman, M., 2005. MMP-1: the elder of the family. Int. J. Biochem. Cell Biol. 37, 283–288. https://doi.org/10.1016/j.biocel.2004.06.017

Pedraz-Petrozzi, B., Insan, S., Spangemacher, M., et al., 2024. Association between rTMS-induced changes in inflammatory markers and improvement in psychiatric diseases: a systematic review. Ann. Gen. Psychiatry 23, 31. https://doi.org/10.1186/s12991-024-00514-0

Poletti, S., Mazza, M.G., Benedetti, F., 2024. Inflammatory mediators in major depression and bipolar disorder. Transl. Psychiatry 14, 247. https://doi.org/10.1038/s41398-024-02921-z

Pramod Shinde, 2021. How is the Limit of Detection (LOD) estimated for OLINK data and how is this handled in the data analysis? - 1st (Internal) Challenge [WWW Document]. CMI-PB Solut. Cent. URL https://discuss.cmi-pb.org/t/how-is-the-limit-of-detection-lod-estimated-for-olink-data-and-how-is-this-handled-in-the-data-analysis/122 (accessed 11.13.25).

Qiu, J., Liu, R., Ma, Y., et al., 2020. Lipopolysaccharide-Induced Depression-Like Behaviors Is Ameliorated by Sodium Butyrate via Inhibiting Neuroinflammation and Oxido-Nitrosative Stress. Pharmacology 105, 550–560. https://doi.org/10.1159/000505132

Raison, C.L., Miller, A.H., 2011. Is Depression an Inflammatory Disorder? Curr. Psychiatry Rep. 13, 467–475. https://doi.org/10.1007/s11920-011-0232-0

Rajkumar, R.P., 2023. Immune-inflammatory markers of response to repetitive transcranial magnetic stimulation in depression: A scoping review. Asian J. Psychiatry 91, 103852. https://doi.org/10.1016/j.ajp.2023.103852

Richards, C.D., 2013. The Enigmatic Cytokine Oncostatin M and Roles in Disease. Int. Sch. Res. Not. 2013, 512103. https://doi.org/10.1155/2013/512103

Schmidt, F.M., Kirkby, K.C., Lichtblau, N., 2016. Inflammation and Immune Regulation as Potential Drug Targets in Antidepressant Treatment. Curr. Neuropharmacol. 14, 674–687. https://doi.org/10.2174/1570159x14666160115130414

Singhal, G., Baune, B.T., 2017. Microglia: An Interface between the Loss of Neuroplasticity and Depression. Front. Cell. Neurosci. 11, 270. https://doi.org/10.3389/fncel.2017.00270

Steiner, J., Guest, P.C., Rahmoune, H., et al., 2017. The Application of Multiplex Biomarker Techniques for Improved Stratification and Treatment of Schizophrenia Patients, in: Guest, P.C. (Ed.), Multiplex Biomarker Techniques: Methods and Applications. Springer, New York, NY, pp. 19–35. https://doi.org/10.1007/978-1-4939-6730-8_2

Strawbridge, R., Arnone, D., Danese, A., et al., 2015. Inflammation and clinical response to treatment in depression: A meta-analysis. Eur. Neuropsychopharmacol. 25, 1532–1543. https://doi.org/10.1016/j.euroneuro.2015.06.007

Strawbridge, R., Hodsoll, J., Powell, T.R., et al., 2019. Inflammatory profiles of severe treatment-resistant depression. J. Affect. Disord. 246, 42–51. https://doi.org/10.1016/j.jad.2018.12.037

Stuart, M.J., Singhal, G., Baune, B.T., 2015. Systematic Review of the Neurobiological Relevance of Chemokines to Psychiatric Disorders. Front. Cell. Neurosci. 9. https://doi.org/10.3389/fncel.2015.00357

Syed, S.A., Beurel, E., Loewenstein, D.A., et al., 2018. Defective Inflammatory Pathways in Never-Treated Depressed Patients Are Associated with Poor Treatment Response. Neuron 99, 914-924.e3. https://doi.org/10.1016/j.neuron.2018.08.001

Tanaka, M., Miyajima, A., 2003. Oncostatin M, a multifunctional cytokine. Rev. Physiol. Biochem. Pharmacol. 149, 39–52. https://doi.org/10.1007/s10254-003-0013-1

Tang, L., Tang, R., Zheng, J., et al., 2025. Dissecting biological heterogeneity in major depressive disorder based on neuroimaging subtypes with multi-omics data. Transl. Psychiatry 15, 72. https://doi.org/10.1038/s41398-025-03286-7

Tayal, U., Verdonschot, J.A.J., Hazebroek, M.R., et al., 2022. Precision Phenotyping of Dilated Cardiomyopathy Using Multidimensional Data. J. Am. Coll. Cardiol. 79, 2219–2232. https://doi.org/10.1016/j.jacc.2022.03.375

Tse, N.Y., Goldsworthy, M.R., Ridding, M.C., et al., 2018. The effect of stimulation interval on plasticity following repeated blocks of intermittent theta burst stimulation. Sci. Rep. 8, 8526. https://doi.org/10.1038/s41598-018-26791-w

Uher, R., Tansey, K.E., Dew, T., et al., 2014. An Inflammatory Biomarker as a Differential Predictor of Outcome of Depression Treatment With Escitalopram and Nortriptyline. Am. J. Psychiatry 171, 1278–1286. https://doi.org/10.1176/appi.ajp.2014.14010094

Voelker, J., Wang, K., Tang, W., et al., 2021. Association of depression symptom severity with short-term risk of an initial hospital encounter in adults with major depressive disorder. BMC Psychiatry 21, 257. https://doi.org/10.1186/s12888-021-03258-3

Voßhenrich, C.A.J., Santo, J.P.D., 2002. Interleukin signaling. Curr. Biol. 12, R760–R763. https://doi.org/10.1016/S0960-9822(02)01286-1

Wang, Q., Zeng, L., Hong, W., et al., 2022. Inflammatory Cytokines Changed in Patients With Depression Before and After Repetitive Transcranial Magnetic Stimulation Treatment. Front. Psychiatry 13, 925007. https://doi.org/10.3389/fpsyt.2022.925007

Wen, X., Aulin, C., Sundberg, E., et al., 2025. Inflammation-profiling reveals activated pathways and biomarkers with predictive potential in oligoarticular juvenile idiopathic arthritis. Front. Immunol. 16, 1599747. https://doi.org/10.3389/fimmu.2025.1599747

Wilkening, J., Goya-Maldonado, R., 2025. White matter tracts associated with iTBS-induced heart rate deceleration and treatment response in major depressive disorder. Transl. Psychiatry 15, 424. https://doi.org/10.1038/s41398-025-03646-3

Wilkening, J., Jungeblut, H.M., Adamovic, I., et al., 2025a. Heart rate modulation and clinical improvement in major depression: A randomized clinical trial with accelerated intermittent theta burst stimulation. Brain Med. 1, 62–72. https://doi.org/10.61373/bm025a.0113

Wilkening, J., Jungeblut, H.M., Adamovic, I., et al., 2025b. Heart rate modulation and clinical improvement in major depression: A randomized clinical trial with accelerated intermittent theta burst stimulation. Brain Med. 1, 62–72. https://doi.org/10.61373/bm025a.0113

Wilkening, J., Witteler, F., Goya-Maldonado, R., 2022. Suicidality and relief of depressive symptoms with intermittent theta burst stimulation in a sham-controlled randomized clinical trial. Acta Psychiatr. Scand. 146, 540–556. https://doi.org/10.1111/acps.13502

World Health Organization, 2017. Depression and other common mental disorders: global health estimates (Technical documents). World Health Organization.

Yang, C., Wardenaar, K.J., Bosker, F.J., et al., 2019. Inflammatory markers and treatment outcome in treatment resistant depression: A systematic review. J. Affect. Disord. 257, 640–649. https://doi.org/10.1016/j.jad.2019.07.045

Yang, L., Cao, M., Tian, J., et al., 2023. Identification of Plasma Inflammatory Markers of Adolescent Depression Using the Olink Proteomics Platform. J. Inflamm. Res. 16, 4489–4501. https://doi.org/10.2147/JIR.S425780

Ye, M., Ji, F., Huang, C., et al., 2024. A novel probiotic formula, BLLL, ameliorates chronic stress-induced depression-like behaviors in mice by reducing neuroinflammation and increasing neurotrophic factors. Front. Pharmacol. 15. https://doi.org/10.3389/fphar.2024.1398292

Yilmaz, N.S., Sen, B., Karadag, R.F., et al., 2022. A kynurenine pathway enzyme aminocarboxymuconate-semialdehyde decarboxylase may be involved in treatment-resistant depression, and baseline inflammation status of patients predicts treatment response: a pilot study. J. Neural Transm. Vienna Austria 1996 129, 1513–1526. https://doi.org/10.1007/s00702-022-02553-x

Yirmiya, R., Goshen, I., 2011. Immune modulation of learning, memory, neural plasticity and neurogenesis. Brain. Behav. Immun. 25, 181–213. https://doi.org/10.1016/j.bbi.2010.10.015

Yoshimura, T., Matsushima, K., Oppenheim, J.J., et al., 1987. Neutrophil chemotactic factor produced by lipopolysaccharide (LPS)-stimulated human blood mononuclear leukocytes: partial characterization and separation from interleukin 1 (IL 1). J. Immunol. Baltim. Md 1950 139, 788–793.

Zimmerman, M., Balling, C., Chelminski, I., et al., 2018. Understanding the severity of depression: Which symptoms of depression are the best indicators of depression severity? Compr. Psychiatry 87, 84–88. https://doi.org/10.1016/j.comppsych.2018.09.006

8. FIGURE LEGENDS

Figure 1 (a–d). Cluster profiles, symptom-level and response-related differences between clusters.

(a) *Cluster profiles based on standardized inflammatory marker expression. The y-axis represents the cluster profiles, and the x-axis shows the z-scores of the 92 inflammatory proteins included in the Olink panel in NPX. The plot illustrates the distinct inflammatory profiles of each cluster derived from k-means clustering.* ***(b)*** *Pie charts showing the proportion of responders and non-responders in each cluster (response defined as ≥50% reduction in MADRS total score); Cluster 2 includes a higher percentage of responders, whereas Cluster 1 includes a higher percentage of non-responders.* ***(c)*** *Bar plot showing cluster-wise mean change in MADRS total score with 95% CIs, illustrating broadly similar overall improvement across clusters.* ***(d)*** *Descriptive radar plot of the mean change (Δ) in individual MADRS item scores from baseline to post-treatment for each cluster. Negative values indicate symptom improvement. Item-level MADRS changes are shown for descriptive purposes only and were not formally compared statistically.*

Figure 2 - Volcano plot of NPX differences between Cluster 1 and Cluster 2.

Vertical blue dotted lines denote NPX differences of +1 and –1. The horizontal red dashed line indicates the FDR-adjusted p-value threshold of 0.05. Abbreviations: NPX = Normalized Protein Expression; IL-7 = Interleukin-7; IL-8 = Interleukin-8; CXCL11 = C-X-C motif chemokine ligand 11; CXCL1 = C-X-C motif chemokine ligand 1; OSM = Oncostatin M; MMP-1 = Matrix metalloproteinase-1; CXCL6 = C-X-C motif chemokine ligand 6; MCP-4 = Monocyte chemotactic protein-4; CXCL5 = C-X-C motif chemokine ligand 5; TNFSF14 = TNF Superfamily Member 14.

Figure 3 - Boxplots of baseline NPX values for ten significantly different inflammatory proteins between Cluster 1 and Cluster 2.

Clusters correspond to patient subgroups with the highest (Cluster 2) versus the lowest (Cluster 1) iTBS response rates; FDR-adjusted p-values are indicated above each plot. Abbreviations: NPX = Normalized Protein Expression; IL-7 = Interleukin-7; IL-8 = Interleukin-8; CXCL11 = C-X-C motif chemokine ligand 11; CXCL1 = C-X-C motif chemokine ligand 1; OSM = Oncostatin M; MMP-1 = Matrix metalloproteinase-1; CXCL6 = C-X-C motif chemokine ligand 6; MCP-4 = Monocyte chemotactic protein-4; CXCL5 = C-X-C motif chemokine ligand 5; TNFSF14 = TNF Superfamily Member 14.

Figure 4 - KEGG and Reactome pathway enrichment analyses.

(a) KEGG pathway enrichment results. The x-axis represents the GeneRatio (the proportion of genes within each pathway that overlap with the list of differentially expressed proteins). Bubble size indicates the number of overlapping genes, while color corresponds to the adjusted p-value (FDR). (b) Reactome pathway enrichment results. The plot displays the enriched biological pathways identified by Reactome analysis. Bubble size reflects the number of genes associated with each path, and color denotes the adjusted p-value. Pathways with similar biological functions are clustered together.

9. TABLES

***Table 1**. General and clinical characteristics of the two-cluster solution (derived from baseline inflammatory profiles), including statistical comparisons across groups. Data are presented as mean (SD) or counts. Group differences were assessed using T-tests or chi-squared tests. Response was defined as ≥50% reduction in MADRS score from baseline. Marked in bold are p-values less than or equal to 0.05.*
Abbreviations: BMI = body mass index, AD = antidepressants; MADRS = Montgomery–Åsberg Depression Rating Scale; SSRI = selective serotonin reuptake inhibitors.

Variable	Total (N = 54)	Cluster 1 (n = 28)	Cluster 2 (n = 26)	p-value	Test type
Age, years	34.50 (12.67)	36.29 (13.44)	32.58 (11.75)	0.287	T-test
Sex, female/male	26/28	14/14	12/14	0.777	Chi-squared
BMI, kg/m^2	25.70 (4.73)	26.80 (5.07)	24.56 (4.15)	0.122	T-test
Baseline MADRS	26.44 (5.03)	26.57 (4.92)	26.31 (5.23)		
Post-treatment MADRS	16.46 (9.52)	18.46 (9.37)	14.31 (9.39)		
ΔMADRS (post-baseline)	-9.98 (10.70)	-8.11 (10.06)	-12.00 (11.20)	0.184	T-test
Randomization order (active-sham/sham-active)				0.176	Chi-squared
Sham first	28	17	11		
Active first	26	11	15		
Treatment resistance				0.700	Chi-squared
Yes	18	18	18		
No	36	10	8		
Current medication				0.897	Chi-squared
No medication	19	10	9		
Medication, non-AD	3	1	2		
Other AD (non-SSRI)	18	9	9		
SSRI	14	8	6		
Response (MADRS ≥ 50%)				**0.031**	Chi-squared
Responders	23	8	15		
Non-responders	31	20	11		

10. FIGURES

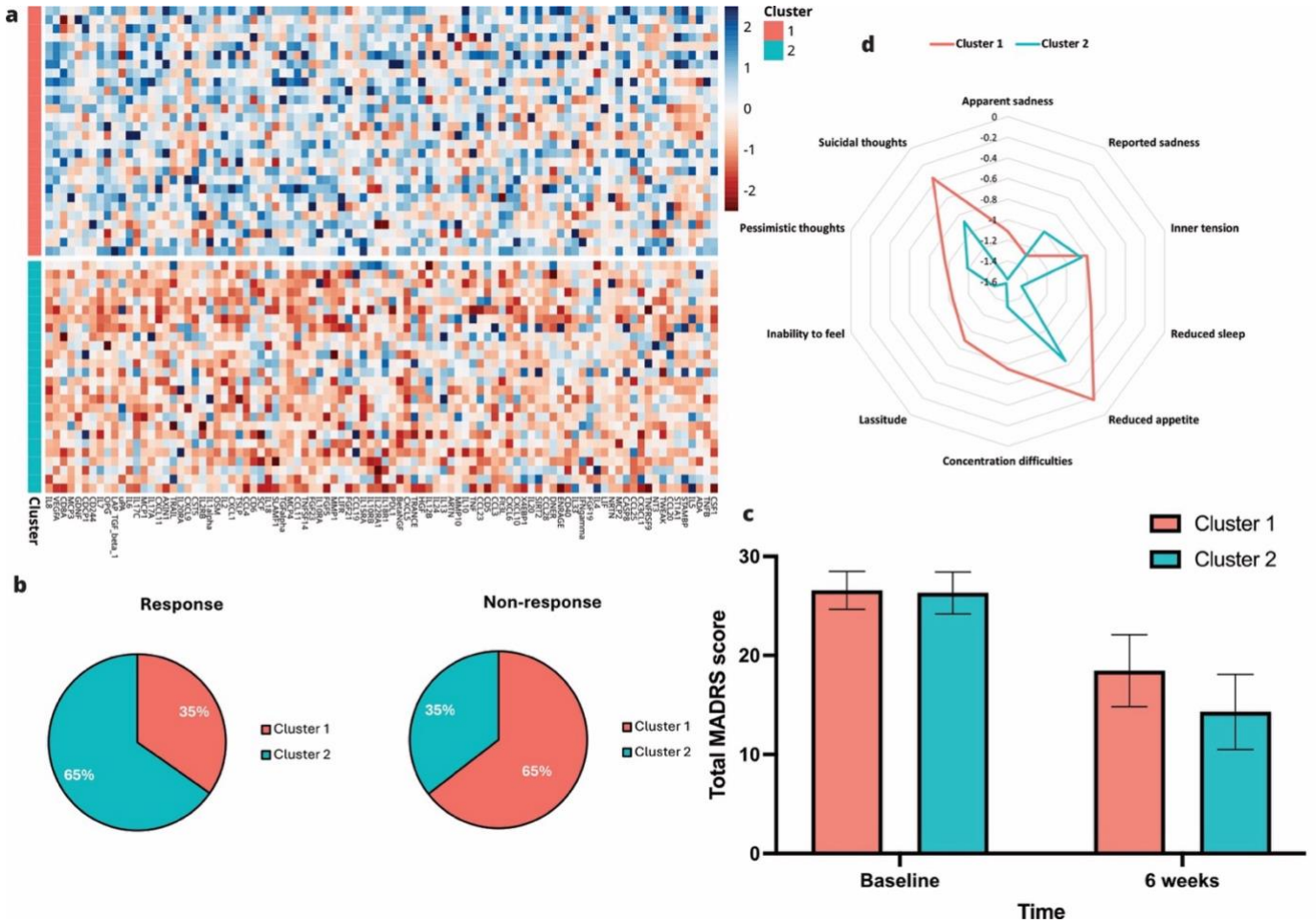

Figure 1 (a–d). Cluster profiles, symptom-level and response-related differences between clusters.

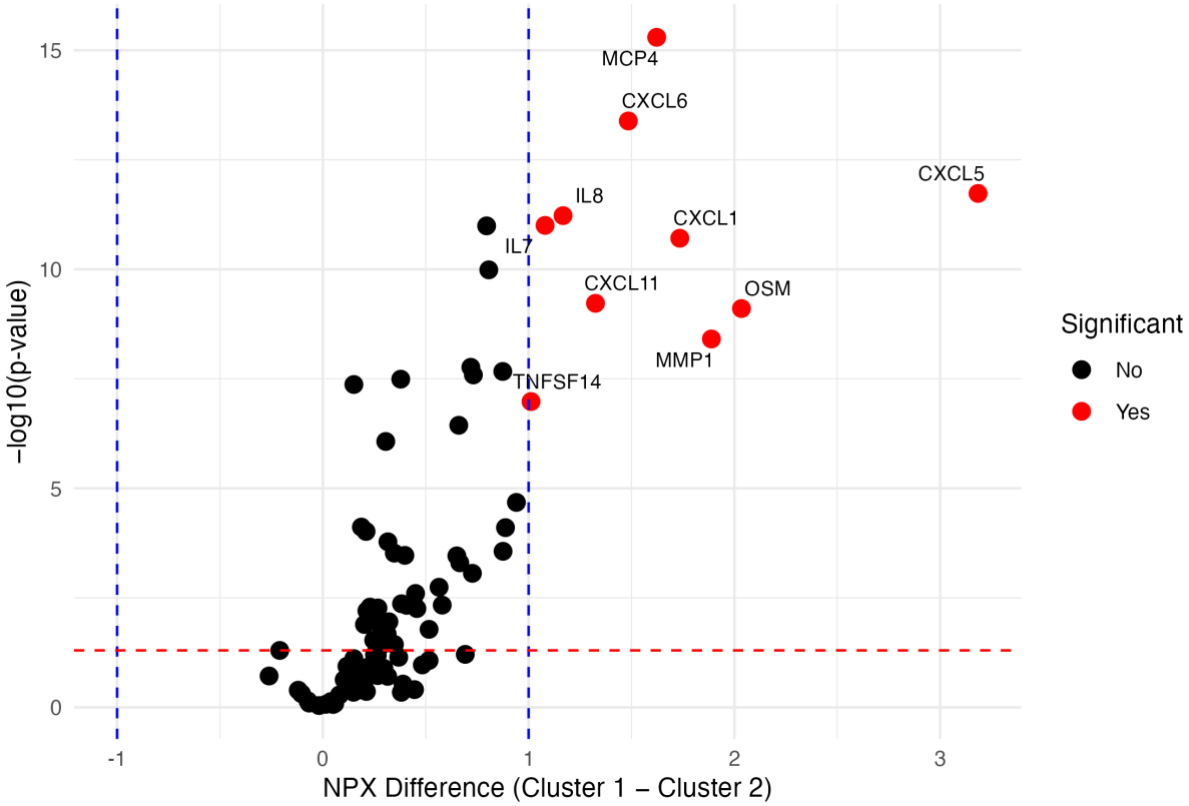

Figure 2 - Volcano plot of NPX differences between Cluster 1 and Cluster 2.

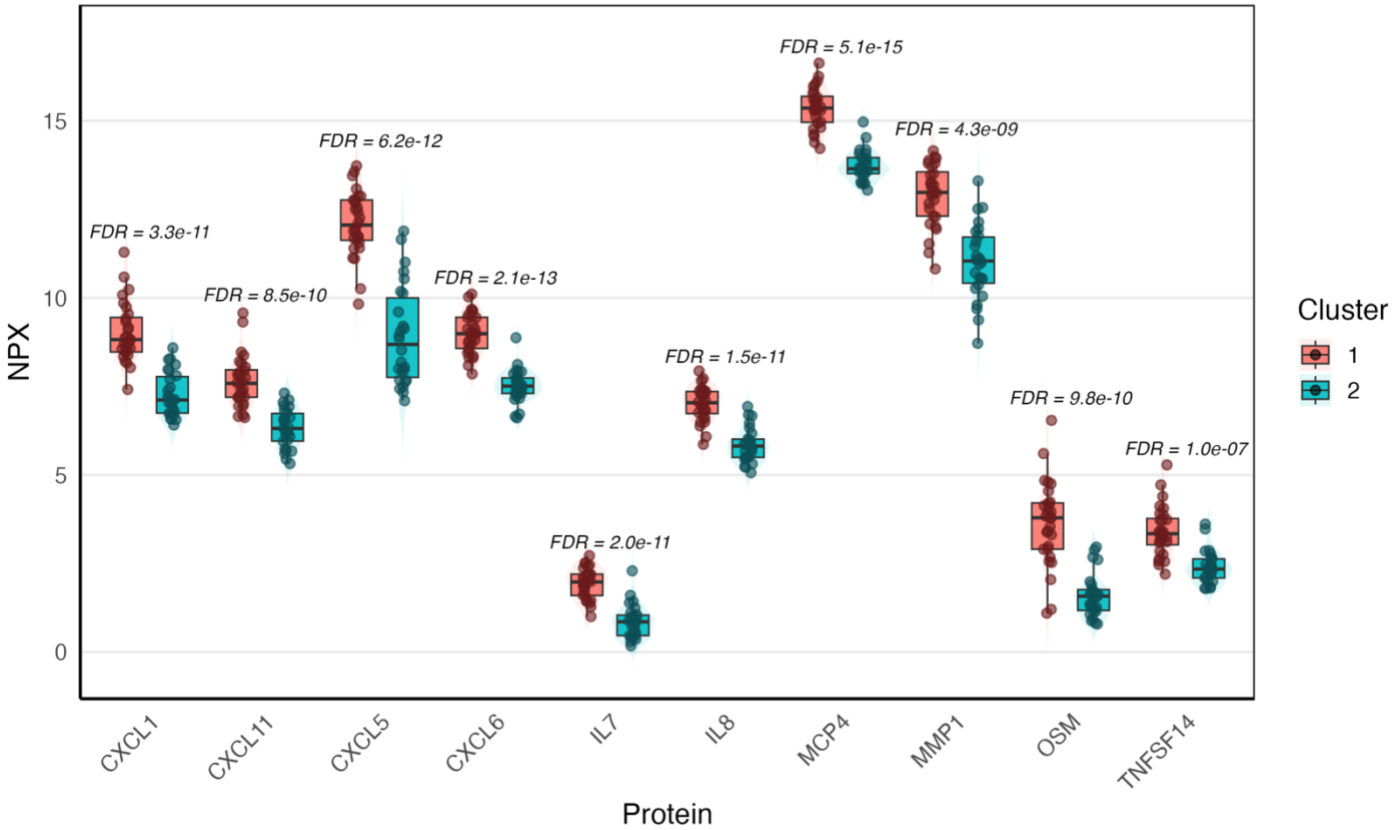

Figure 3 - Boxplots of baseline NPX values for ten significantly different inflammatory proteins between Cluster 1 and Cluster 2.

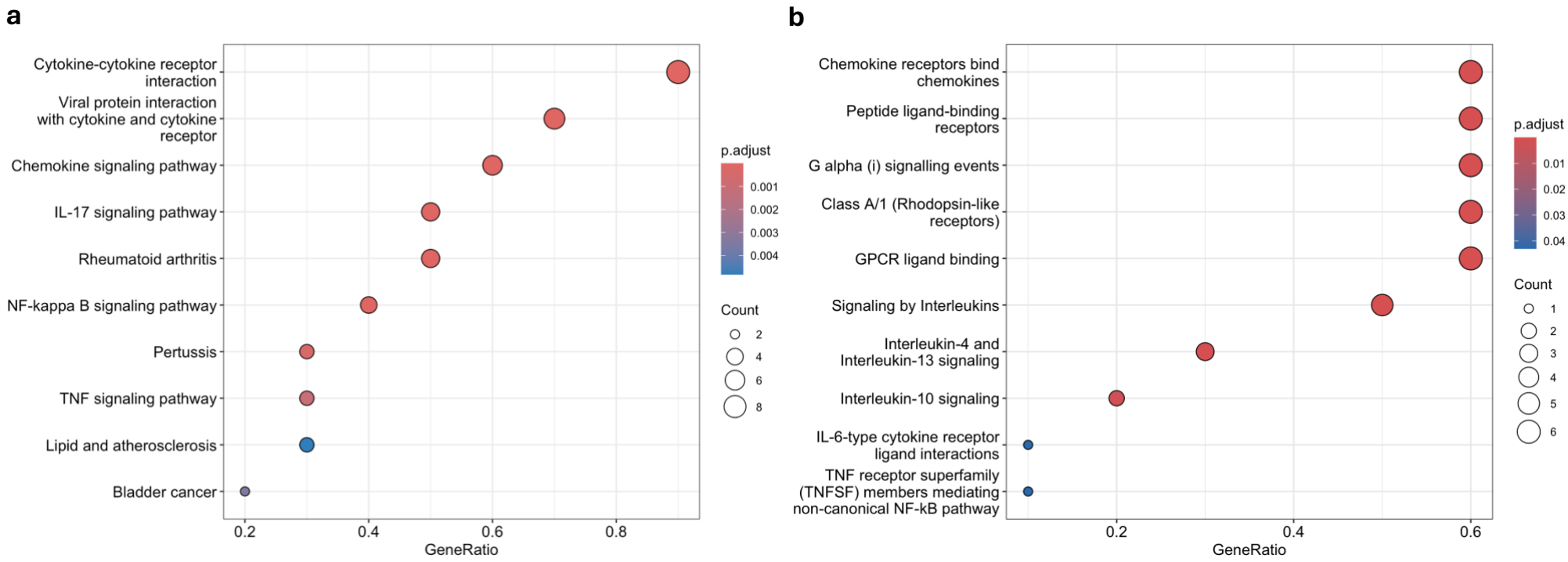

Figure 4 - KEGG and Reactome pathway enrichment analyses.

SUPPLEMENTAL MATERIAL 1

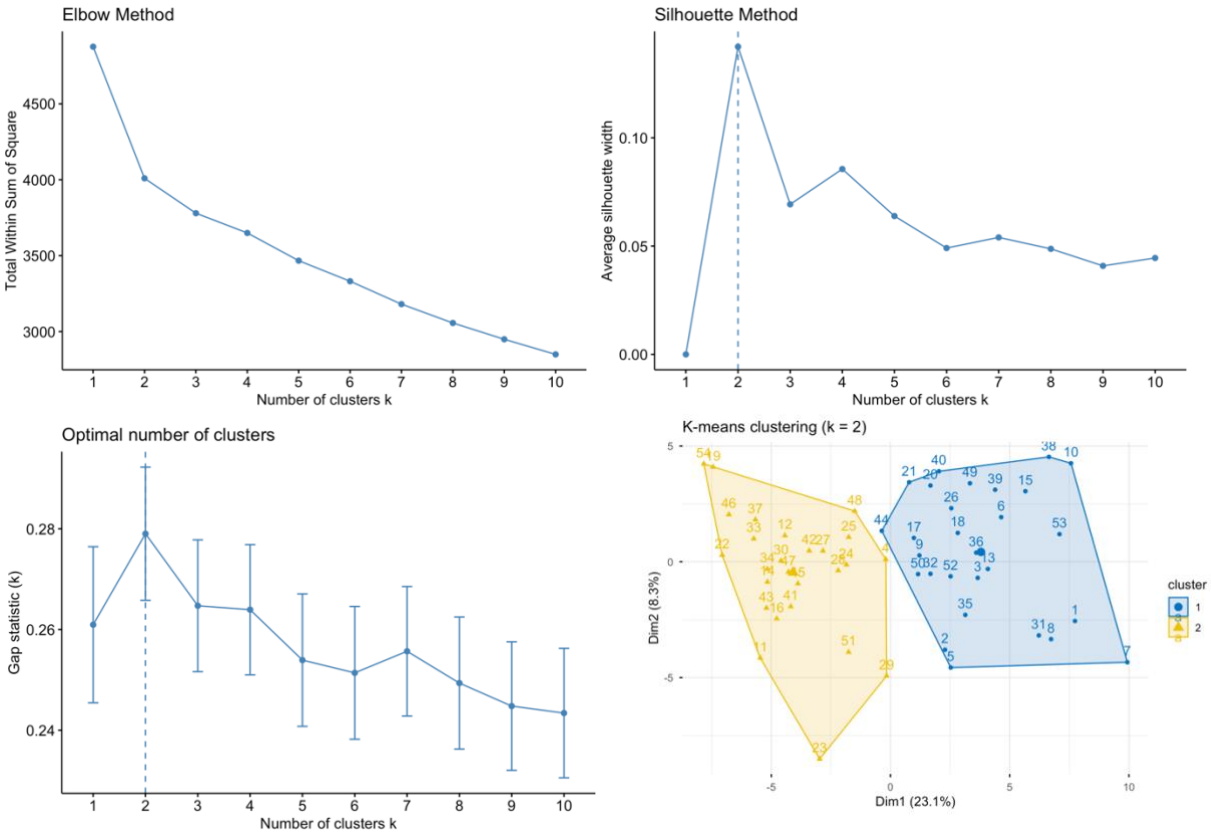

Supplementary Figure 1. *Exploratory cluster validity diagnostics using the Elbow, Gap Statistics, and Silhouette methods. All metrics were computed for k values ranging from 1 to 10, based on the standardized expression of inflammatory proteins. All methods suggest a cluster solution of k = 2.*

Table S1. *Distribution of medication category across inflammatory clusters and responder groups*

Medication category	Non-responder, n	Responder, n
No medication	9	10
Non-antidepressant medication	3	0
Other antidepressants than SSRIs	11	7
SSRI	8	6

Table S2. *Baseline Medication load by cluster and responder status. Medication-load comparisons were performed using Wilcoxon rank-sum tests. P-values are from Wilcoxon rank-sum tests.*

Variable	Group	n	Mean	SD	p-value
Baseline medication load	Cluster 1	28	1.64	1.79	0.934
Baseline medication load	Cluster 2	26	1.62	1.88	
Baseline medication load	Non-responder	31	1.71	1.83	0.592
Baseline medication load	Responder	23	1.52	1.83	

Table S3. *Firth penalized logistic regression models examining medication-related confounding of the association between inflammatory cluster membership and treatment response. Odds ratios (ORs), 95% confidence intervals (CIs), and p-values are from Firth penalized logistic regression models with responder status as the dependent variable. Medication was coded as no medication (at all), non-antidepressant medication, antidepressants other than SSRIs, and SSRIs.*

Model	Term	OR	95% CI	p-value
M0 unadjusted	Cluster 2 vs 1	3.25	1.10–10.20	0.033
M1 adjusted for medication category	Cluster 2 vs 1	3.64	1.21–11.83	0.021
Non-antidepressant medication vs no medication	0.08	0.00–1.18	0.068	
Other antidepressants vs no medication	0.54	0.14–2.03	0.365	
SSRI vs no medication	0.71	0.17–2.91	0.633	
M2 adjusted for baseline medication load	Cluster 2 vs 1	3.19	1.09–9.90	0.034
Baseline medication load	0.95	0.69–1.28	0.734	
M3 adjusted for medication-free vs medicated	Cluster 2 vs 1	3.30	1.11–10.48	0.031
Medicated vs medication-free	0.51	0.16–1.61	0.252	

Table S4. *Proteins showing significant differences in expression between Cluster 1 and Cluster 2 (|ΔNPX| ≥ 1.0 and FDR < 0.05). Effect sizes are reported as Cohen's d, Hedges' g, and Glass's Δ for each cluster. All proteins achieved post-hoc power > 0.999.*

Significant Protein	Cohen's d	Hedges' g	Glass Delta - Cluster 1	Glass Delta - Cluster 2	Power
IL8	2.41	2.38	2.40	2.42	1.000
IL7	2.40	2.36	2.52	2.29	1.000
CXCL11	2.06	2.03	1.84	2.42	1.000
OSM	2.12	2.09	1.70	3.32	1.000
CXCL1	2.32	2.29	2.05	2.79	1.000
MCP4	3.18	3.13	2.82	3.79	1.000
TNFSF14	1.68	1.66	1.43	2.19	1.000
MMP1	1.96	1.94	2.18	1.79	1.000
CXCL5	2.70	2.66	3.45	2.27	1.000
CXCL6	2.79	2.75	2.57	3.10	1.000

Table S5. *KEGG Pathway Enrichment Analysis - This table presents the results of KEGG pathway enrichment analysis performed on the differentially expressed proteins. Pathways are identified by KEGG ID and grouped by category. The columns display the gene ratio, background ratio, enrichment scores, p-values, and the corresponding genes.*

KEGG ID	Category	Subcategory	Description	GeneRatio	BgRatio	RichFactor	FoldEnrichment	Z-score	p-value	p.adjust	q-value
hsa04060	Environmental Information Processing	Signaling molecules and interaction	Cytokine-cytokine receptor interaction	9/10	298/9497	0.030201342	28.68221477	15.76320628	2.54843E-13	9.93887E-12	5.36511E-12
hsa04061	Environmental Information Processing	Signaling molecules and interaction	Viral protein interaction with cytokine and cytokine receptor	7/10	100/9497	0.07	66.479	21.37043328	1.35698E-12	2.64611E-11	1.4284E-11
hsa04062	Organismal Systems	Immune system	Chemokine signaling pathway	6/10	193/9497	0.031088083	29.52435233	12.99766976	1.2796E-08	1.66348E-07	8.97968E-08
hsa04657	Organismal Systems	Immune system	IL-17 signaling pathway	5/10	95/9497	0.052631579	49.98421053	15.57807157	2.18207E-08	1.70201E-07	9.18766E-08
hsa05323	Human Diseases	Immune disease	Rheumatoid arthritis	5/10	95/9497	0.052631579	49.98421053	15.57807157	2.18207E-08	1.70201E-07	9.18766E-08
hsa04064	Environmental Information Processing	Signal transduction	NF-kappa B signaling pathway	4/10	105/9497	0.038095238	36.17904762	11.76807935	2.81546E-06	1.83005E-05	9.8788E-06
hsa05133	Human Diseases	Infectious disease: bacterial	Pertussis	3/10	78/9497	0.038461538	36.52692308	10.22841643	6.13635E-05	0.000341882	0.000184552
hsa04668	Environmental Information Processing	Signal transduction	TNF signaling pathway	3/10	119/9497	0.025210084	23.94201681	8.176282017	0.00021589	0.001052464	0.000568132
hsa05219	Human Diseases	Cancer: specific types	Bladder cancer	2/10	41/9497	0.048780488	46.32682927	9.442770603	0.000800592	0.003469232	0.00187273
hsa05417	Human Diseases	Cardiovascular disease	Lipid and atherosclerosis	3/10	216/9497	0.013888889	13.19027778	5.883679315	0.001237208	0.004825112	0.002604649
hsa05134	Human Diseases	Infectious disease: bacterial	Legionellosis	2/10	56/9497	0.035714286	33.91785714	8.020888396	0.001490928	0.005286016	0.00285345
hsa05120	Human Diseases	Infectious disease: bacterial	Epithelial cell signaling in Helicobacter pylori infection	2/10	71/9497	0.028169014	26.75211268	7.071055129	0.002385614	0.007753247	0.004185288

hsa05146	Human Diseases	Infectious disease: parasitic	Amoebiasis	2/10	103/9497	0.019417476	18.4407767	5.777833981	0.004952993	0.01485898	0.008021042
hsa04620	Organismal Systems	Immune system	Toll-like receptor signaling pathway	2/10	109/9497	0.018348624	17.42568807	5.599589396	0.005531149	0.015408201	0.008317518
hsa04936	Human Diseases	Endocrine and metabolic disease	Alcoholic liver disease	2/10	144/9497	0.013888889	13.19027778	4.785477553	0.009486706	0.024665435	0.013314675
hsa04630	Environmental Information Processing	Signal transduction	JAK-STAT signaling pathway	2/10	168/9497	0.011904762	11.30595238	4.375534661	0.012752051	0.031083123	0.016779014
hsa04621	Organismal Systems	Immune system	NOD-like receptor signaling pathway	2/10	189/9497	0.010582011	10.04973545	4.079852866	0.015960392	0.036615016	0.019765191
hsa05167	Human Diseases	Infectious disease: viral	Kaposi sarcoma-associated herpesvirus infection	2/10	196/9497	0.010204082	9.690816327	3.991440758	0.017100324	0.037050701	0.020000378
hsa05171	Human Diseases	Infectious disease: viral	Coronavirus disease - COVID-19	2/10	238/9497	0.008403361	7.980672269	3.540866787	0.024647703	0.050592653	0.027310474
hsa05144	Human Diseases	Infectious disease: parasitic	Malaria	1/10	50/9497	0.02	18.994	4.141633486	0.051442036	0.098902291	0.053388551
hsa04151	Environmental Information Processing	Signal transduction	PI3K-Akt signaling pathway	2/10	362/9497	0.005524862	5.246961326	2.674756295	0.05325508	0.098902291	0.053388551

Table S6. Reactome Pathway Enrichment Analysis - *This table presents the results of Reactome pathway enrichment analysis. The analysis identifies biological pathways significantly enriched among differentially expressed proteins. Key metrics include gene ratios, enrichment factors, and statistical significance values.*

Reactome ID	Description	GeneRatio	BgRatio	RichFactor	FoldEnrichment	Z-score	p-value	p.adjust	q-value
R-HSA-380108	Chemokine receptors bind chemokines	6/10	59/11214	0.101694915	114.040678	26.00760335	3.37506E-12	9.11265E-11	3.55269E-11
R-HSA-375276	Peptide ligand-binding receptors	6/10	201/11214	0.029850746	33.47462687	13.87917781	6.08992E-09	8.22139E-08	3.20522E-08
R-HSA-418594	G alpha (i) signalling events	6/10	318/11214	0.018867925	21.15849057	10.89462744	9.46826E-08	8.52143E-07	3.3222E-07
R-HSA-373076	Class A/1 (Rhodopsin-like receptors)	6/10	334/11214	0.017964072	20.14491018	10.61173705	1.26766E-07	8.55671E-07	3.33595E-07
R-HSA-500792	GPCR ligand binding	6/10	468/11214	0.012820513	14.37692308	8.831411051	9.31783E-07	5.03163E-06	1.96165E-06
R-HSA-449147	Signaling by Interleukins	5/10	460/11214	0.010869565	12.18913043	7.320902068	2.41389E-05	0.000108625	4.2349E-05
R-HSA-6785807	Interleukin-4 and Interleukin-13 signaling	3/10	108/11214	0.027777778	31.15	9.405777926	9.92488E-05	0.000382817	0.000149246
R-HSA-6783783	Interleukin-10 signaling	2/10	47/11214	0.042553191	47.71914894	9.58848415	0.000757331	0.002555993	0.000996488
R-HSA-6788467	IL-6-type cytokine receptor ligand interactions	1/10	17/11214	0.058823529	65.96470588	8.008025717	0.015062627	0.043044131	0.016781338
R-HSA-5676594	TNF receptor superfamily (TNFSF) members mediating non-canonical NF-kB pathway	1/10	18/11214	0.055555556	62.3	7.775702628	0.015942271	0.043044131	0.016781338
R-HSA-6783589	Interleukin-6 family signaling	1/10	24/11214	0.041666667	46.725	6.699133813	0.021205303	0.049025857	0.019113395
R-HSA-210991	Basigin interactions	1/10	25/11214	0.04	44.856	6.55809565	0.022080008	0.049025857	0.019113395
R-HSA-380994	ATF4 activates genes in response to endoplasmic reticulum stress	1/10	27/11214	0.037037037	41.53333333	6.299582157	0.023827307	0.049025857	0.019113395
R-HSA-5669034	TNFs bind their physiological receptors	1/10	29/11214	0.034482759	38.66896552	6.067909003	0.025571796	0.049025857	0.019113395
R-HSA-381042	PERK regulates gene expression	1/10	32/11214	0.03125	35.04375	5.761386343	0.02818327	0.049025857	0.019113395
R-HSA-1592389	Activation of Matrix Metalloproteinases	1/10	33/11214	0.03030303	33.98181818	5.66846671	0.02905236	0.049025857	0.019113395
R-HSA-1266695	Interleukin-7 signaling	1/10	36/11214	0.027777778	31.15	5.412910861	0.031655435	0.050276279	0.019600889
R-HSA-1442490	Collagen degradation	1/10	64/11214	0.015625	17.521875	3.959918488	0.055649646	0.08347447	0.032543653

SUPPLEMENTAL MATERIAL 2:

***Table S1**. Differential inflammatory protein expression between Clusters 1 and 2. Log_2 fold change (log2FC), t-statistics, p-values, false discovery rate (FDR, Benjamini–Hochberg correction), and $-log_{10}(p)$ values are shown. Proteins meeting both thresholds (FDR < 0.05 and $|log_2FC| \geq 1$) are marked as significant.*

Protein	log2FC	Welch's t	P-value	FDR	negLog10P	Significant
MCP4	**1.62245703**	**11.8009548**	**5.0639E-16**	**4.6588E-14**	**15.2955138**	**Yes**
CXCL6	**1.4846631**	**10.3125154**	**4.1172E-14**	**1.8939E-12**	**13.3853936**	**Yes**
CXCL5	**3.18426113**	**9.76934379**	**1.8562E-12**	**5.6923E-11**	**11.7313762**	**Yes**
IL8	**1.16732495**	**8.85867253**	**5.9613E-12**	**1.3711E-10**	**11.2246607**	**Yes**
IL7	**1.07997137**	**8.77162243**	**9.9632E-12**	**1.5641E-10**	**11.0015997**	**Yes**
CXCL1	**1.73495228**	**8.62831032**	**1.9549E-11**	**2.5693E-10**	**10.7088818**	**Yes**
CXCL11	**1.32497332**	**7.63995951**	**5.9745E-10**	**6.1072E-09**	**9.22370204**	**Yes**
OSM	**2.03457387**	**7.9527285**	**7.8756E-10**	**7.2456E-09**	**9.10371641**	**Yes**
MMP1	**1.88841591**	**7.16190465**	**3.897E-09**	**3.2593E-08**	**8.40927236**	**Yes**
TNFSF14	**1.01165525**	**6.27282862**	**1.0448E-07**	**5.654E-07**	**6.98098679**	**Yes**
VEGFA	0.79586876	9.10932163	1.0201E-11	1.5641E-10	10.9913753	No
MCP1	0.80640052	8.10039153	1.0296E-10	1.1841E-09	9.98732503	No
HGF	0.71906113	6.70427436	1.7258E-08	1.3231E-07	7.76300132	No
CCL4	0.87426396	6.63820717	2.1484E-08	1.5204E-07	7.66788369	No
LAP_TGF_beta_1	0.7315919	6.97457185	2.5766E-08	1.6932E-07	7.58895211	No
CD40	0.37847676	6.49138499	3.2244E-08	1.9776E-07	7.49154978	No
BetaNGF	0.15075687	6.4229248	4.2658E-08	2.4529E-07	7.3699967	No
CCL11	0.6605053	5.82479758	3.6363E-07	1.8585E-06	6.4393418	No
CSF1	0.30567912	5.5946875	8.5155E-07	4.1233E-06	6.06978964	No
MCP2	0.94065206	4.71782064	2.0957E-05	9.6403E-05	4.67866812	No
LIFR	0.18724717	4.29748115	7.6606E-05	0.00033028	4.11573865	No
CCL28	0.88765038	4.37237123	7.898E-05	0.00033028	4.10248425	No
FGF5	0.20991316	4.28018995	9.6393E-05	0.00038557	4.01595558	No
IL2	0.31612923	4.05996065	0.00016614	0.00063687	3.77952239	No
AXIN1	0.87560536	3.92463465	0.00027376	0.00100743	3.56263229	No
TWEAK	0.3473425	3.88527928	0.00030188	0.00106818	3.52017078	No
TGFalpha	0.65109459	4.02798177	0.00034778	0.00114272	3.45869103	No
FGF23	0.39848085	3.84195352	0.00033869	0.00114272	3.47019312	No
IL6	0.66537577	3.79005774	0.00050107	0.00158961	3.30009909	No
MCP3	0.7267847	3.56390063	0.00087053	0.00266964	3.0602143	No
CXCL10	0.56474739	3.29553749	0.00181002	0.00537166	2.74231736	No
IL18	0.45034981	3.19199748	0.00251083	0.00721865	2.60018203	No
CD244	0.38222725	3.04128775	0.00430929	0.01177884	2.36559469	No
TSLP	0.44179071	2.9820517	0.00435305	0.01177884	2.36120624	No
CD8A	0.40727777	2.95644299	0.00468573	0.01197465	2.32922263	No

CCL3	0.58003874	3.01023253	0.00463335	0.01197465	2.33410446	No
IL10RB	0.22937753	2.92268739	0.00513938	0.012779	2.28908918	No
IL20	0.26767492	2.96739644	0.00538362	0.01303403	2.26892552	No
LIF	0.45684736	2.94447094	0.00554268	0.01307504	2.25628017	No
SCF	0.2560839	2.86339675	0.00626671	0.01406189	2.20296026	No
IL15RA	0.21398549	2.85707692	0.00624672	0.01406189	2.204348	No
CX3CL1	0.25930467	2.70380015	0.00943074	0.02065781	2.02545429	No
TNF	0.32097132	2.64104313	0.01110024	0.02374935	1.9546676	No
OPG	0.20219635	2.58566133	0.01282976	0.02682586	1.89178142	No
IL24	0.51616451	2.52233776	0.01655235	0.03384036	1.78114037	No
CCL23	0.28418264	2.41699114	0.01921881	0.03843762	1.71627354	No
CCL25	0.31237016	2.38025012	0.02100899	0.04112397	1.67759492	No
PDL1	0.24700615	2.24434464	0.02926184	0.0560852	1.53369835	No
CXCL9	0.34765467	2.15224695	0.0365743	0.06794211	1.43682398	No
IL10	0.28845382	2.14380487	0.03692506	0.06794211	1.4326788	No
IL13	-0.209523	-2.0179745	0.05018665	0.09053277	1.29941182	No
FGF21	0.69206808	1.91201311	0.06164143	0.10905792	1.21012727	No
ARTN	0.25103168	1.90535453	0.06285128	0.10910033	1.2016859	No
TNFB	0.26447846	1.89328199	0.06505792	0.11083941	1.18669985	No
IL22RA1	0.36874838	1.83833152	0.07179225	0.12008885	1.14392245	No
TNFRSF9	0.15054766	1.80756572	0.0770854	0.1266403	1.11302787	No
ST1A1	0.51608514	1.76418689	0.08490655	0.13704216	1.07105878	No
ENRAGE	0.48332918	1.63889722	0.10733062	0.17024856	0.96927638	No
CD5	0.13097813	1.60259035	0.1151057	0.17692435	0.93890318	No
DNER	0.11703228	1.60123179	0.11538544	0.17692435	0.93784898	No
CST5	0.21866937	1.57891383	0.12045871	0.18167543	0.91916179	No
SLAMF1	0.14080396	1.55580891	0.12589204	0.18680755	0.90000172	No
CASP8	0.29678404	1.54479664	0.12886259	0.18818029	0.88987315	No
IL2RB	0.14173981	1.42331167	0.16108615	0.23156135	0.79294179	No
IL33	0.14325019	1.40819906	0.1654665	0.23419874	0.78128991	No
CDCP1	0.19470022	1.39163693	0.1711456	0.23856659	0.76663426	No
IL17C	0.26826775	1.35828864	0.18033822	0.2476286	0.74391223	No
GDNF	0.26576385	1.34034435	0.18816982	0.25458269	0.72545004	No
CCL19	-0.2611943	-1.3301976	0.19206595	0.25608794	0.71654962	No
CCL20	0.31484203	1.31105296	0.19567584	0.25717396	0.70846279	No
Flt3L	0.12100423	1.26920897	0.2100702	0.27220364	0.67763556	No
TRAIL	0.10361879	1.20690134	0.23388507	0.29885315	0.6309975	No
MMP10	0.19843277	1.06970647	0.29026749	0.36537421	0.5372016	No
STAMBP	0.38922135	1.06049327	0.29388795	0.36537421	0.53181822	No
NT3	0.18215407	0.96575663	0.3386376	0.41539546	0.47026482	No
IL12B	0.12438008	0.93818187	0.3526866	0.42693641	0.45261104	No

X4EBP1	0.4453519	0.8609896	0.39328861	0.46990327	0.40528863	No
NRTN	0.17649157	0.84930049	0.39976256	0.47151481	0.39819788	No
IL4	-0.1196149	-0.8406157	0.40530293	0.47199835	0.39222025	No
IFNgamma	0.21160107	0.79099878	0.43312321	0.49809169	0.36338854	No
IL10RA	0.14897665	0.75811684	0.45180459	0.5072877	0.34504936	No
SIRT2	0.38127637	0.75766049	0.45214773	0.5072877	0.34471964	No
IL20RA	-0.1034946	-0.7039539	0.48661771	0.53938349	0.31281209	No
IL1alpha	0.08059563	0.64695249	0.52051413	0.5700869	0.28356748	No
TRANCE	-0.0722001	-0.3711834	0.71230634	0.77096687	0.14733319	No
IL18R1	0.03845277	0.33541954	0.73878028	0.79032309	0.1314847	No
CD6	0.03922107	0.31572324	0.75347654	0.79677979	0.12293026	No
IL5	-0.0665603	-0.2570105	0.7982658	0.83455061	0.09785248	No
IL17A	0.05758302	0.23093774	0.8184289	0.84601639	0.08701904	No
uPA	0.01343049	0.18698556	0.85239968	0.86673509	0.06935672	No
FGF19	0.04971769	0.18068911	0.85731406	0.86673509	0.06686006	No
ADA	-0.0187937	-0.1172451	0.90713743	0.90713743	0.04232691	No

ABBREVIATION LIST

4E-BP1	Eukaryotic Translation Initiation Factor 4E-Binding Protein 1
ADA	Adenosine Deaminase
ARTN	Artemin
AXIN1	Axis Inhibition Protein 1
Beta-NGF	Beta Nerve Growth Factor
BMI	Body Mass Index
CASP-8	Caspase 8
CCL11	C-C Motif Chemokine Ligand 11 (Eotaxin-1)
CCL19	C-C Motif Chemokine Ligand 19
CCL20	C-C Motif Chemokine Ligand 20
CCL23	C-C Motif Chemokine Ligand 23
CCL25	C-C Motif Chemokine Ligand 25
CCL28	C-C Motif Chemokine Ligand 28
CCL3	C-C Motif Chemokine Ligand 3
CCL4	C-C Motif Chemokine Ligand 4
CD244	CD244 Molecule (2B4)
CD40	CD40 Molecule
CD5	CD5 Molecule
CD6	CD6 Molecule
CD8A	CD8a Molecule
CDCP1	CUB Domain Containing Protein 1
CNS	Central Nervous System
CRP	C-Reactive Protein
CSF-1	Colony Stimulating Factor 1
CST5	Cystatin D
CX3CL1	CX3C Motif Chemokine Ligand 1 (Fractalkine)
CXC	C-X-C Motif Chemokine Family

CXCL	C-X-C Motif Chemokine Ligand (e.g., CXCL1, CXCL5, CXCL6, CXCL11)
CXCL1	C-X-C Motif Chemokine Ligand 1
CXCL10	C-X-C Motif Chemokine Ligand 10
CXCL11	C-X-C Motif Chemokine Ligand 11
CXCL5	C-X-C Motif Chemokine Ligand 5
CXCL6	C-X-C Motif Chemokine Ligand 6
CXCL9	C-X-C Motif Chemokine Ligand 9
DEPs	Differentially Expressed Proteins
DLPFC	Dorsolateral Prefrontal Cortex
DNER	Delta/Notch-Like EGF Repeat Containing
DSM-5	Diagnostic and Statistical Manual of Mental Disorders, Fifth Edition
ECT	Electroconvulsive Therapy
EDTA	Ethylenediaminetetraacetic Acid
EN-RAGE	Extracellular Newly Identified RAGE-Binding Protein (S100A12)
FDA	U.S. Food and Drug Administration
FDR	False Discovery Rate
FGF-19	Fibroblast Growth Factor 19
FGF-21	Fibroblast Growth Factor 21
FGF-23	Fibroblast Growth Factor 23
FGF-5	Fibroblast Growth Factor 5
Flt3L	FMS-like Tyrosine Kinase 3 Ligand
GDNF	Glial Cell Line-Derived Neurotrophic Factor
gp130	Glycoprotein 130
GPCR	G-Protein–Coupled Receptor
HGF	Hepatocyte Growth Factor
HPA	Hypothalamic–Pituitary–Adrenal Axis
IFNγ	Interferon Gamma

IL	Interleukin (e.g., IL-6, IL-8, IL-10, IL-13)
IL10RA	Interleukin 10 Receptor Subunit Alpha
IL10RB	Interleukin 10 Receptor Subunit Beta
IL12B	Interleukin 12 Subunit Beta
IL15RA	Interleukin 15 Receptor Alpha
IL17A	Interleukin 17A
IL17C	Interleukin 17C
IL18R1	Interleukin 18 Receptor 1
IL1α	Interleukin 1 Alpha
IL1β	Interleukin 1 Beta
IL20	Interleukin 20
IL20RA	Interleukin 20 Receptor Alpha
IL22RA1	Interleukin 22 Receptor Subunit Alpha 1
IL24	Interleukin 24
IL2RB	Interleukin 2 Receptor Subunit Beta
IL6	Interleukin 6
IL10	Interleukin 10
IL13	Interleukin 13
IL18	Interleukin 18
IL2	Interleukin 2
IL33	Interleukin 33
IL4	Interleukin 4
IL5	Interleukin 5
IL7	Interleukin 7
IL8	Interleukin 8
ITAC	Interferon-inducible T-cell Alpha Chemoattractant
iTBS	Intermittent Theta Burst Stimulation
JAK/STAT	Janus Kinase/Signal Transducer and Activator of Transcription Pathway

KEGG	Kyoto Encyclopedia of Genes and Genomes
LAP TGF-beta-1	Latency-Associated Peptide of TGF-β1
LIF	Leukemia Inhibitory Factor
LIF-R	Leukemia Inhibitory Factor Receptor
MADRS	Montgomery–Åsberg Depression Rating Scale
MAPK	Mitogen-Activated Protein Kinase
MCP	Monocyte Chemotactic Protein
MCP-1	Monocyte Chemoattractant Protein 1 (CCL2)
MCP-2	Monocyte Chemoattractant Protein 2 (CCL8)
MCP-3	Monocyte Chemoattractant Protein 3 (CCL7)
MCP-4	Monocyte Chemoattractant Protein 4 (CCL13)
MDD	Major Depressive Disorder
MMP	Matrix Metalloproteinase (e.g., MMP-1)
MMP-1	Matrix Metallopeptidase 1
MMP-10	Matrix Metallopeptidase 10
MRI	Magnetic Resonance Imaging
NF-κB	Nuclear Factor Kappa-Light-Chain-Enhancer of Activated B Cells
NPX	Normalized Protein Expression (Olink Platform Metric)
NRTN	Neurturin
NT-3	Neurotrophin-3
OPG	Osteoprotegerin (TNFRSF11B)
OSM	Oncostatin M
PD-L1	Programmed Death-Ligand 1 (CD274)
PEA	Proximity Extension Assay
pMADRS	Percentage Change in MADRS Item
RMT	Resting Motor Threshold
rTMS	Repetitive Transcranial Magnetic Stimulation
SCF	Stem Cell Factor (KITLG)

SCID-5-CV	Structured Clinical Interview for DSM-5 Disorders – Clinical Version
SD	Standard Deviation
SIRT2	Sirtuin 2
SLAMF1	SLAM Family Member 1
ST1A1	Sulfotransferase Family 1A Member 1
STAMBP	STAM Binding Protein
STAT3	Signal Transducer and Activator of Transcription 3
tENS	Transcutaneous Electrical Nerve Stimulation
TGF-alpha	Transforming Growth Factor Alpha
TNF	Tumor Necrosis Factor
TNF-α	Tumor Necrosis Factor Alpha
TNFB	Tumor Necrosis Factor Beta (Lymphotoxin Alpha)
TNFRSF9	TNF Receptor Superfamily Member 9 (4-1BB/CD137)
TNFSF14	TNF Superfamily Member 14 (LIGHT)
TRAIL	TNF-Related Apoptosis-Inducing Ligand (TNFSF10)
TRANCE	TNF-Related Activation-Induced Cytokine (RANKL/TNFSF11)
TSLP	Thymic Stromal Lymphopoietin
TWEAK	TNF-Like Weak Inducer of Apoptosis (TNFSF12)
uPA	Urokinase-type Plasminogen Activator
VEGFA	Vascular Endothelial Growth Factor A
ΔMADRS	Change in MADRS Score (post-treatment minus baseline)

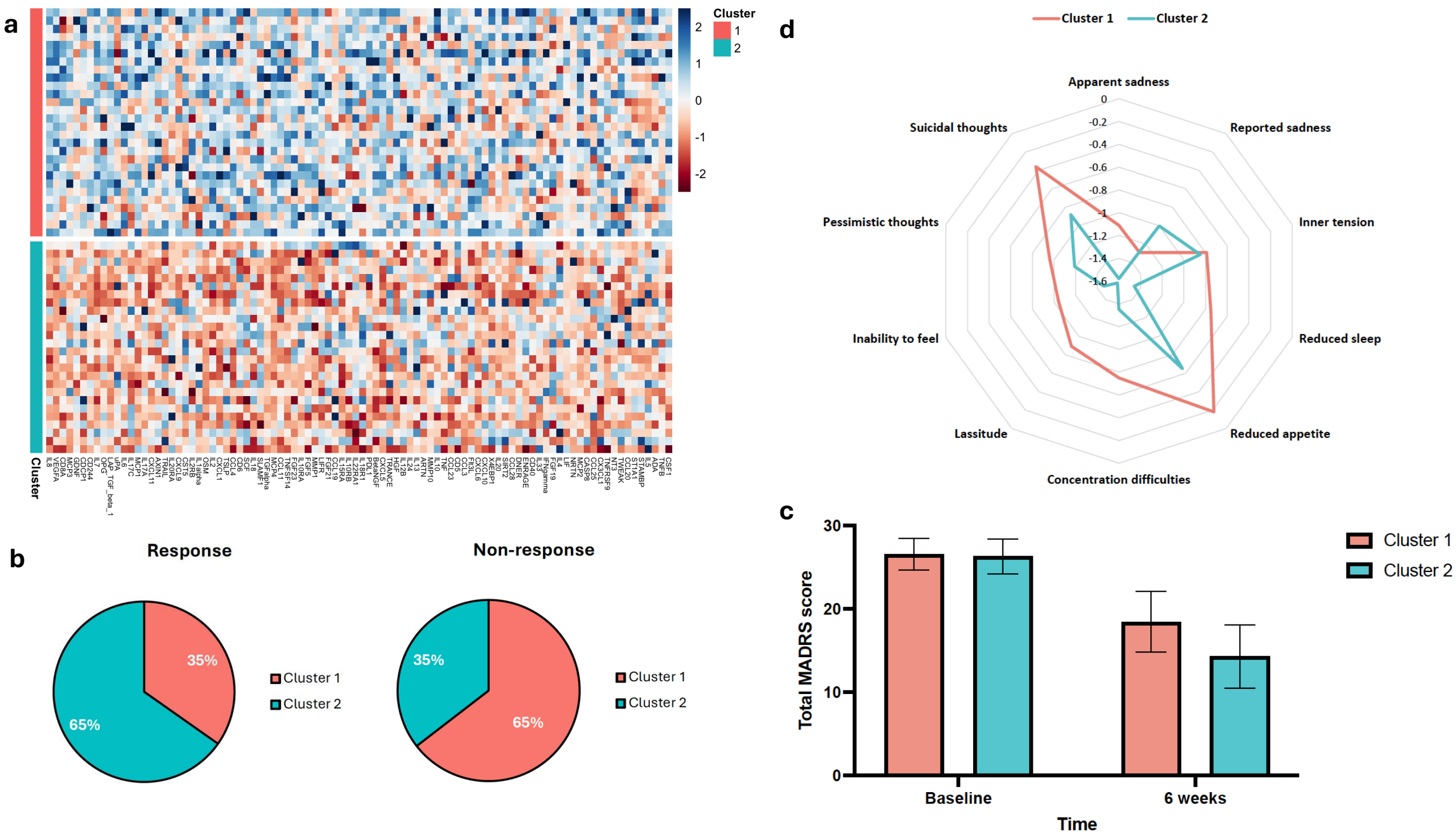
a
Cluster
1
2
2
1
0
-1
-2
Cluster
b
Response
35%
65%
Cluster 1
Cluster 2
Non-response
35%
65%
Cluster 1
Cluster 2
c
Total MADRS score
30
20
10
0
Baseline
6 weeks
Time
Cluster 1
Cluster 2
d
Cluster 1
Cluster 2
Apparent sadness
Reported sadness
Inner tension
Reduced sleep
Reduced appetite
Concentration difficulties
Lassitude
Inability to feel
Pessimistic thoughts
Suicidal thoughts
0
-0.2
-0.4
-0.6
-0.8
-1
-1.2
-1.4
-1.6

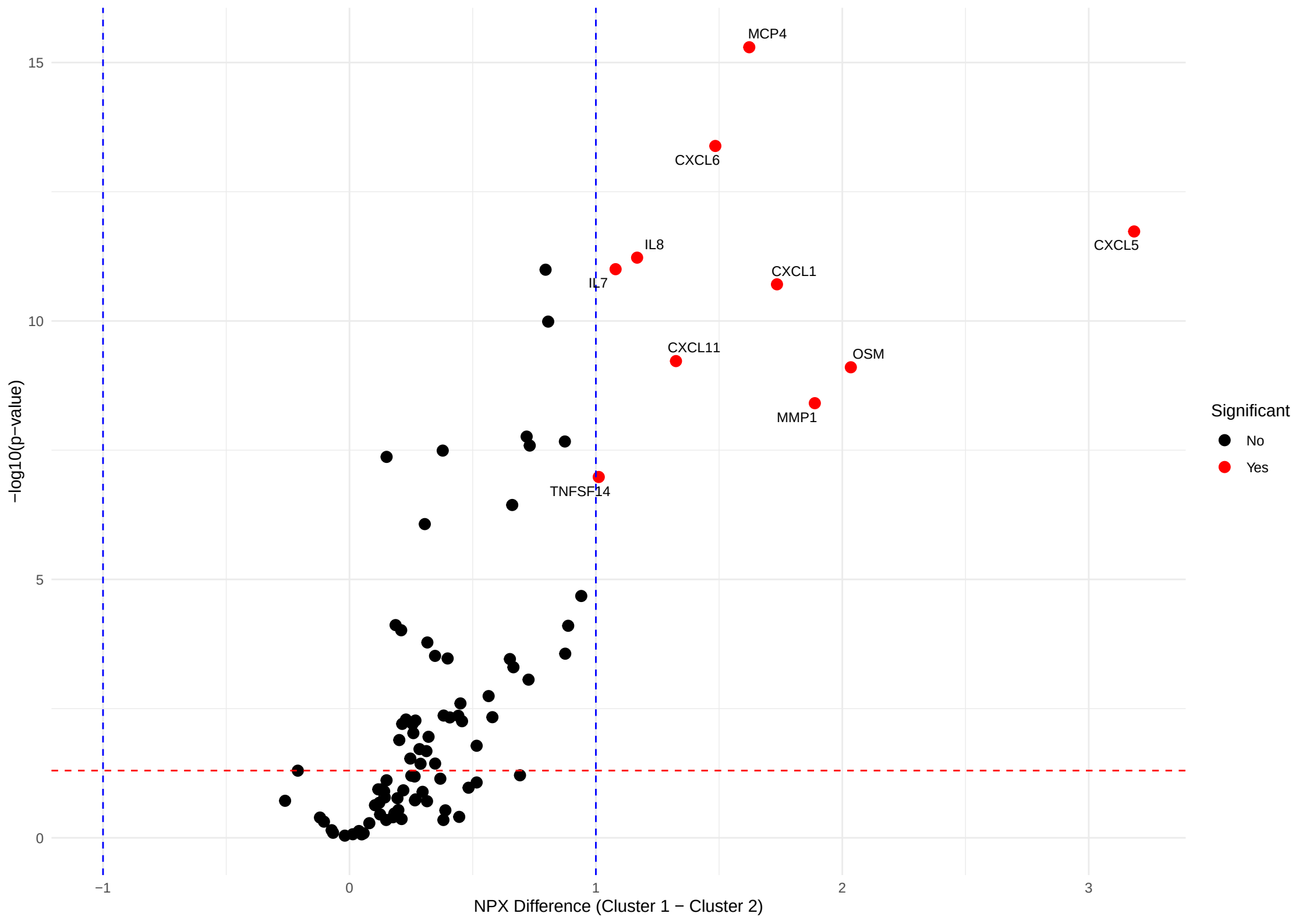
MCP4
CXCL6
CXCL5
IL8
IL7
CXCL1
CXCL11
OSM
MMP1
TNFSF14
15
10
5
0
−1
0
1
2
3
−log10(p−value)
NPX Difference (Cluster 1 − Cluster 2)
Significant
No
Yes

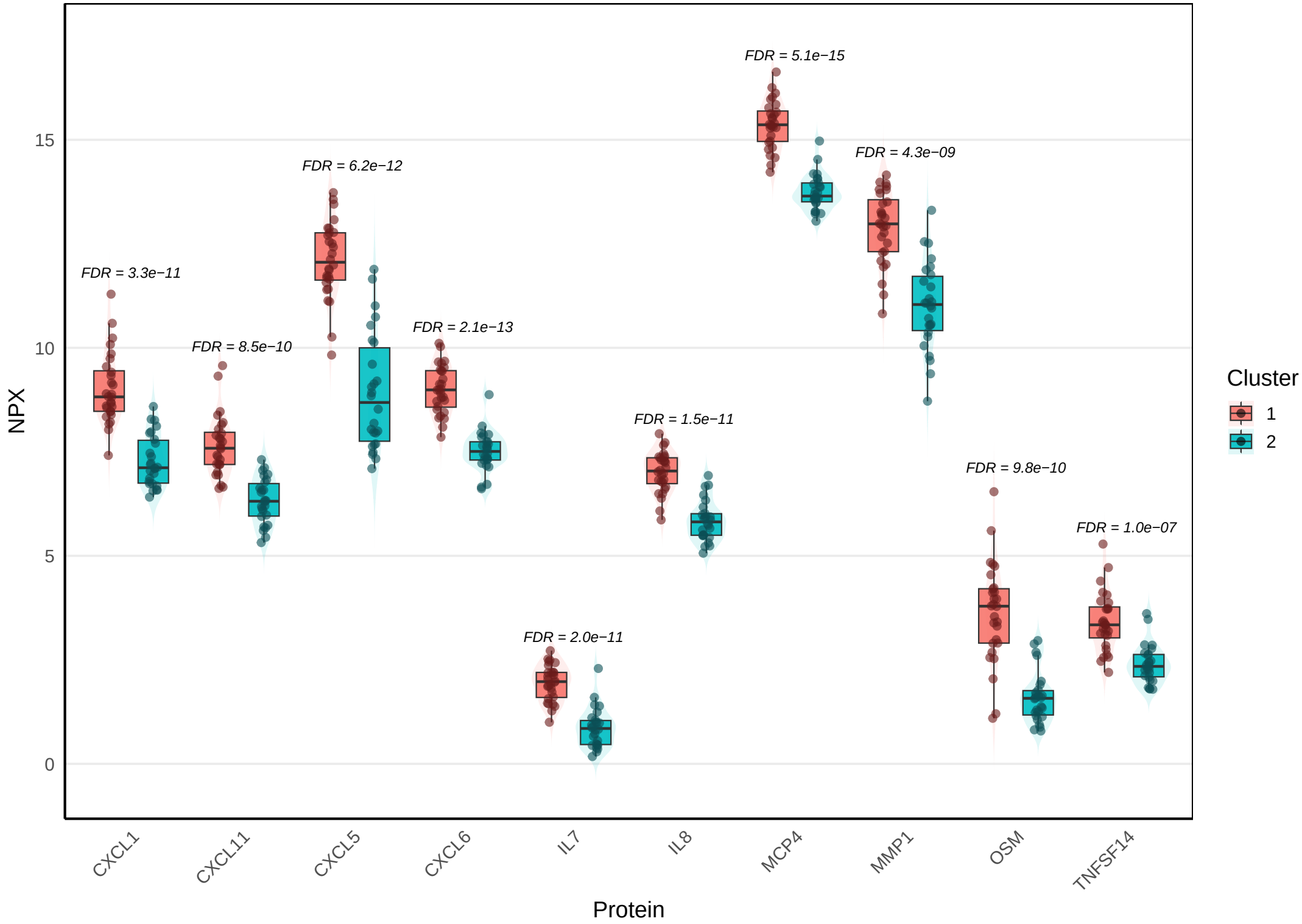
FDR = 3.3e−11
FDR = 8.5e−10
FDR = 6.2e−12
FDR = 2.1e−13
FDR = 2.0e−11
FDR = 1.5e−11
FDR = 5.1e−15
FDR = 4.3e−09
FDR = 9.8e−10
FDR = 1.0e−07
NPX
15
10
5
0
CXCL1
CXCL11
CXCL5
CXCL6
IL7
IL8
MCP4
MMP1
OSM
TNFSF14
Protein
Cluster
1
2

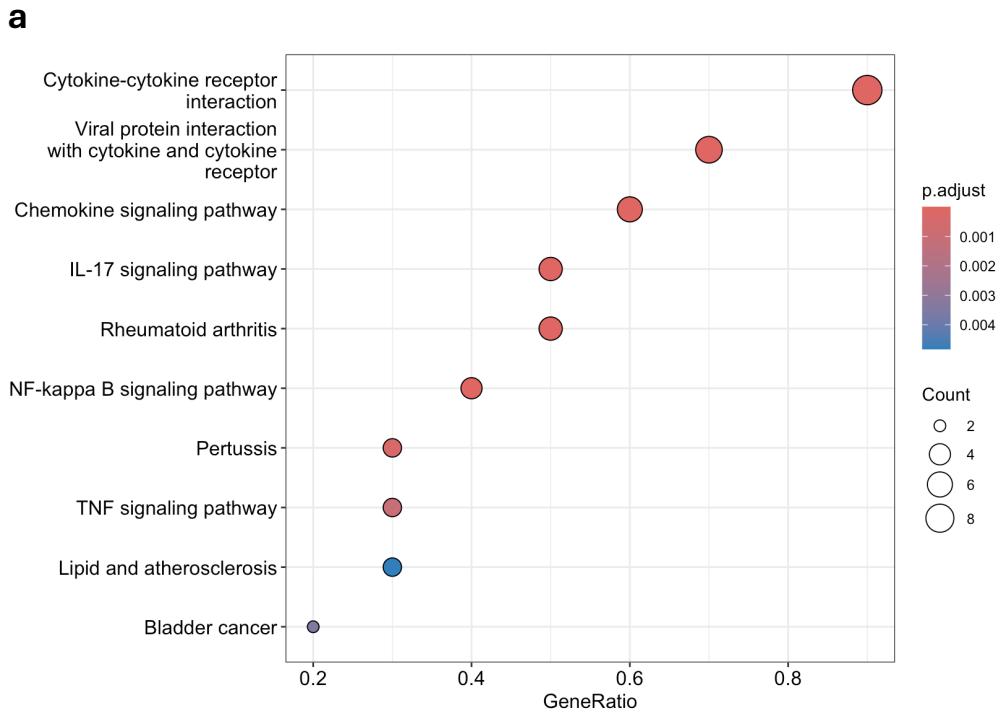
a
Cytokine-cytokine receptor interaction
Viral protein interaction with cytokine and cytokine receptor
Chemokine signaling pathway
IL-17 signaling pathway
Rheumatoid arthritis
NF-kappa B signaling pathway
Pertussis
TNF signaling pathway
Lipid and atherosclerosis
Bladder cancer
0.2
0.4
0.6
0.8
GeneRatio
p.adjust
0.001
0.002
0.003
0.004
Count
2
4
6
8

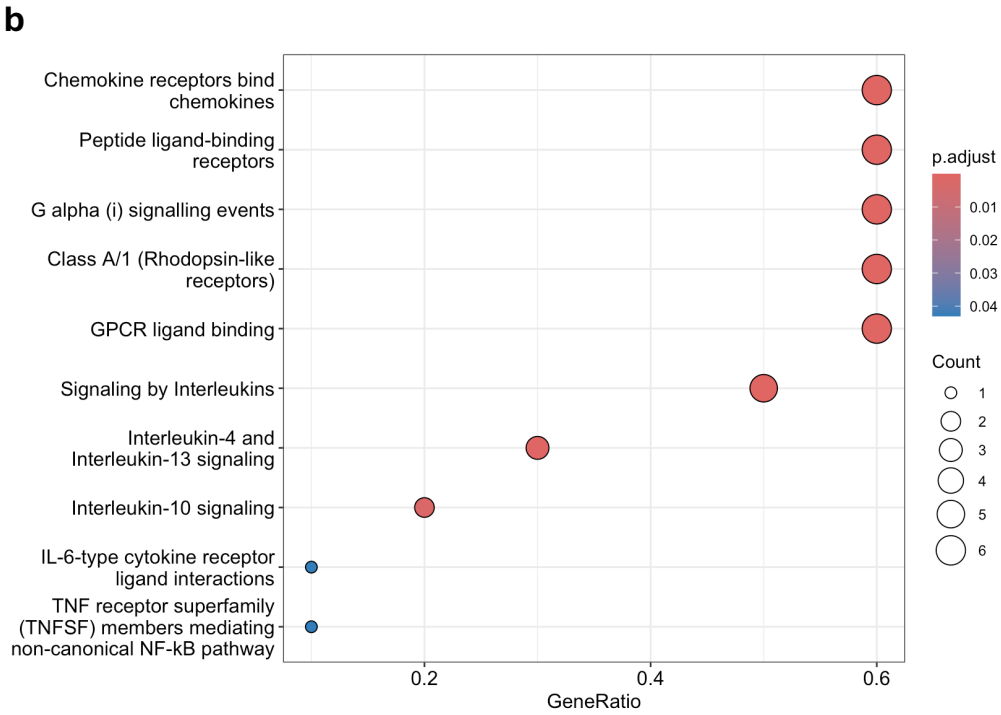
b
Chemokine receptors bind chemokines
Peptide ligand-binding receptors
G alpha (i) signalling events
Class A/1 (Rhodopsin-like receptors)
GPCR ligand binding
Signaling by Interleukins
Interleukin-4 and Interleukin-13 signaling
Interleukin-10 signaling
IL-6-type cytokine receptor ligand interactions
TNF receptor superfamily (TNFSF) members mediating non-canonical NF-kB pathway
0.2
0.4
0.6
GeneRatio
p.adjust
0.01
0.02
0.03
0.04
Count
1
2
3
4
5
6